Journal of Asian Earth Sciences xxx (2012) xxx–xxx

Contents lists available at SciVerse ScienceDirect

Journal of Asian Earth Sciences

journal homepage: www.elsevier.com/locate/jseaes

Review

Pleistocene alluvial deposits dating along frontal thrust of Changhua Fault in western Taiwan: The cosmic ray exposure point of view

Lionel L. Siame [a,h,*], Rou-Fei Chen [b,c,h], Florence Derrieux [a], Jian-Cheng Lee [b,h], Kuo-Jen Chang [d,h], Didier L. Bourlès [a,h], Régis Braucher [a,h], Laetitia Léanni [a], Chu-Chun Kang [e], Chung-Pai Chang [e,f,h], Hao-Tsu Chu [g,h]

[a] Centre Européen de Recherche et d'Enseignement en Géosciences de l'Environnement (CEREGE) – UMR 7330 CNRS-INSU, Aix-Marseille Université, IRD, BP 80, Plateau de l'Arbois, 13545 Aix-en-Provence cedex 4, France
[b] Institute of Earth Sciences, Academia Sinica, 128 Academia Road, Sec. 2, Nankang, Taipei 115, Taiwan
[c] Department of Geology, Chinese Culture University, 55, Hwa-Kang Road, Yang-Ming-Shan, Taipei, Taiwan
[d] Department of Civil Engineering, National Taipei University of Technology, Taipei 106, Taiwan
[e] Institute of Geophysics, National Central University, Jhongli, Taoyuan, Taiwan
[f] Center for Space and Remote Sensing Research, National Central University, 300, Jhongda Road, Jhongli, Taoyuan, Taiwan
[g] Central Geological Survey, Ministry of Economic Affairs, P.O. Box 968, Taipei, Taiwan
[h] LIA (Associated International Laboratory), ADEPT (Active Deformation and Environment Programme for Taiwan), Centre National de la Recherche Scientifique/Institut National des Sciences de l'Univers (France), National Science Council (Taiwan)

ARTICLE INFO

Article history:
Received 3 September 2011
Received in revised form 19 January 2012
Accepted 8 February 2012
Available online xxxx

Keywords:
Cosmogenic nuclides
Alluvial deposits
Active tectonics
Seismic hazards

ABSTRACT

To tackle the history of active thrusts, it is necessary to open the observation window on time scales on the order of 10^4–10^5 years by studying the surface morphologies resulting from their activities. Because fluvial systems are particularly sensitive to recent environmental changes, geomorphic features such as alluvial terraces are frequently used as markers to gauge tectonic deformation. Together with the measurement of cumulative displacements, the chronological framework of emplacement and abandonment of these geomorphic markers is thus fundamental to determine long-term fault slip-rates. In Taiwan, the geomorphic features associated with fault activity have been studied in detail with a high level of resolution; however, the use of deformed and partially preserved alluvial terraces is often hampered by the absence of well-documented ages. The purpose of this paper is two-fold. First, we take the opportunity to review the chronological constraints that have been published in Taiwan so far. Second, we present how the cosmogenic dating method (in situ-produced ^{10}Be) can be used to constraint the chronological framework of alluvial deposits over a Pleistocene time scale. Thanks to a comparison of our cosmogenic-derived ages with existing data, we present a consistent regional chronological framework for the Pakua–Tadu area along the Changhua Fault, one of the most active frontal thrusts in the Western Foothills of the Taiwan mountain belt. We also discuss its relationships with global eustatism and its tectonic implications for the timing of propagation of the deformation front during the last 450 kyr.

Contents

* Corresponding author at: Centre Européen de Recherche et d'Enseignement en Géosciences de l'Environnement (CEREGE) – UMR 7330 CNRS-INSU, Aix-Marseille Université, IRD, BP 80, Plateau de l'Arbois, 13545 Aix-en-Provence cedex 4, France. Tel.: +33 442 971 760.
E-mail address: siame@cerege.fr (L.L. Siame).

1367-9120/$ - see front matter © 2012 Elsevier Ltd. All rights reserved.
doi:10.1016/j.jseaes.2012.02.002

1. Introduction

At the plate tectonic scale, there is an overall agreement between far-field geodetic deformation rates and geological plate velocities derived from seafloor spreading since 3 Ma (DeMets et al., 1990, 1994, 2010). Within this context, interplate fault slip rates are usually considered as constant due to steady plate boundary loading rates. However, on individual fault systems, comparisons of geological and geodetic fault slip rates suggest that they may have varied over long-spanned time scales (Grant and Sieh, 1994; Stein et al., 1997; Bendick et al., 2000; Dawson et al., 2003; Dixon et al., 2002; Friedrich et al., 2003; Ryerson et al., 2006). Measurements and comparison of fault slip rates integrated over different time spans are thus important not only to apprehend how plate convergence is accommodated by continental lithospheres but also to determine to what extend the slip rate variations may be related to the fault strength or to the transient accumulation of elastic strain in the lithosphere (*e.g.*, Fay and Humphreys, 2005; Oskin et al., 2007; Chuang and Johnson, 2011).

To measure deformation rates of active tectonics, geoscientists use a number of tools spanning very different time scales. Over decadal time scales, leveling, Global Positioning System (GPS) and more recently Interferometry Synthetic Aperture Radar (InSAR) techniques (Massonnet and Feil, 1998; Burgmann et al., 2000) allow constraining velocity fields and determining slip rates either on individual faults or at the regional scale (Holt et al., 2000; Huang et al., 2009; Wei et al., 2011; Walters et al., 2011). Together with geodetic measurements, earthquake moment summations also allow calculating regional strain-released rates (Westaway, 1992; Siame et al., 2005; Mouthereau et al., 2009; Walker et al., 2010). To investigate the representativeness of current rates, it is necessary to open the observation window of crustal deformation on time scales typically spanning several tens to several hundreds of thousand years (*i.e.*, over the Pleistocene to Late Quaternary). For such time scales, geomorphic offset measurements and dated features allows determining averaged fault slip rates. Over the last two decades, this morpho-chronometric approach has been facilitated by development of dating methods such as Optically-Stimulated Luminescence (OSL) and Cosmic Ray Exposure (CRE) techniques, which allow reaching time spans far beyond radiocarbon dating (*i.e.*, older than 45 ky), and in regions where radiocarbon-datable materials are not available or difficult to obtain.

Among the geomorphic markers that can be used to gauge the deformation cumulated over the Holocene or the Pleistocene, fluvial terraces constitute well-suited features that are particularly sensitive to climate variations, sea level changes and/or tectonic forcing to which they systematically adjust (Schumm, 1977; Avouac and Peltzer, 1993; Merritts et al., 1994; Pazzaglia et al., 1998; Maddy et al., 2001; Bridgland and Westaway, 2008; Lu et al., 2010). In compressional settings such as piedmonts of active fold-and-thrust belts, the relief growth due to the tectonic deformation frequently interferes with the geomorphic impact of fluvial activity on landscapes (e.g., Molnar et al., 1994; Yang et al., 2011). Within such contexts, the combination of surface uplift, river deposition and subsequent incision creates geomorphic features that are generally characterized by stepped, abandoned fluvial terraces while progressively uplifted, folded and/or tilted. As a result, dating fluvial terraces became a common method to estimate rates of active tectonics.

In this article, we focused on the terrace deposits in the frontal thrust zone of the Taiwan mountain belt, which is related to the oblique collision between the Philippine Sea and Eurasian plates (Fig. 1). In Taiwan, recent geodetic surveys using Global Positioning System (GPS) showed that in the central part of the Taiwan mountains, the plate suture in the eastern side (Coastal Range and Longitudinal Valley) and the Western Foothills both account for nearly 50% (3–4 cm/year) of the plate convergence rate, respectively (Yu et al., 1997; Hsu et al., 2009). To investigate whether such rates of deformation are representative on millennial time scales, we focused on the landscape development in relation with the Changhua Fault, one of the major frontal thrusts in western Taiwan (Fig. 1). In the Western Foothills, the tectonic deformation is seemingly closely related to the abundant late Quaternary alluvial deposits that skirt the piedmont of the mountain belt. This paper is thus taking the opportunity to review the chronological constraints that have been published so far and to present how we used the cosmogenic dating method (in situ-produced ^{10}Be) to constraint the chronological framework of alluvial deposits over a Pleistocene time scale. Thanks to a comparison of our cosmogenic-derived ages with existing data such as pedogenic characteristics of the alluvial deposits, we propose a consistent chronological framework for fluvial terraces emplacement in the Pakua–Tadu region. We also discuss its relationships with global eustatism and its tectonic implications for the timing of propagation of the deformation front since about 450 kyr.

2. Geodynamic and geological contexts

Taiwan is recognized as one of the best places in the world to address major questions regarding mechanisms of deformation in convergent settings, processes of mountain building (from oceanic subduction to continental subduction and post-orogenic extension), and subsequent active deformation involving several significant seismogenic faults (Fig. 1). Taiwan is located at the boundary between the Eurasian and Philippine Sea plates, and makes the junction between the Ryukyu and the Manila, two opposing trench systems. Along the Ryukyu trench, the Philippine

Please cite this article in press as: Siame, L.L., et al. Pleistocene alluvial deposits dating along frontal thrust of Changhua Fault in western Taiwan: The cosmic ray exposure point of view. Journal of Asian Earth Sciences (2012), doi:10.1016/j.jseaes.2012.02.002

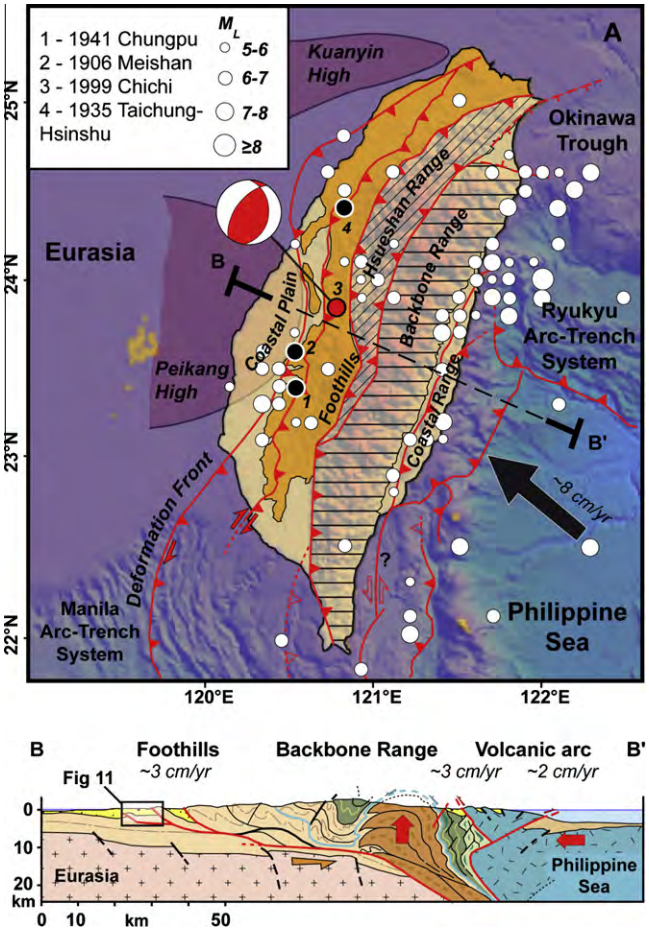

Fig. 1. (A) Tectonic framework and main structural units of the Taiwan collision zone (after Angelier et al. (2009)). Large arrow indicates the plate convergence direction of Philippine Sea plate relative to Eurasia (Sella et al., 2002). Open circles locate earthquakes with ML ⩾ 5 (1900–2006; Central Weather Bureau of Taiwan, Ng et al., 2009). Solid circles locate Western Foothills' largest destructive earthquakes: 1906 Meishan (ML = 7.1, depth = 6 km), 1935 Taichung-Hsinchu (ML = 7.1, depth = 5 km), 1941 Chungpu (ML = 7.1, depth = 12 km) and 1999 Chi–Chi (ML = 7.3, depth = 8 km). The focal mechanism of the Chi–Chi mainshock is after Chang et al. (2000). (B) Section across the orogen showing the main zones of active faulting and exhumation (after Malavieille (2010)). Numbers refer to short-term shortening estimates through the deformation front (Simoes and Avouac, 2006), the Longitudinal Valley (Angelier et al., 2000; Shyu et al., 2006) and offshore within the Philippine Sea plate (Malavieille et al., 2002).

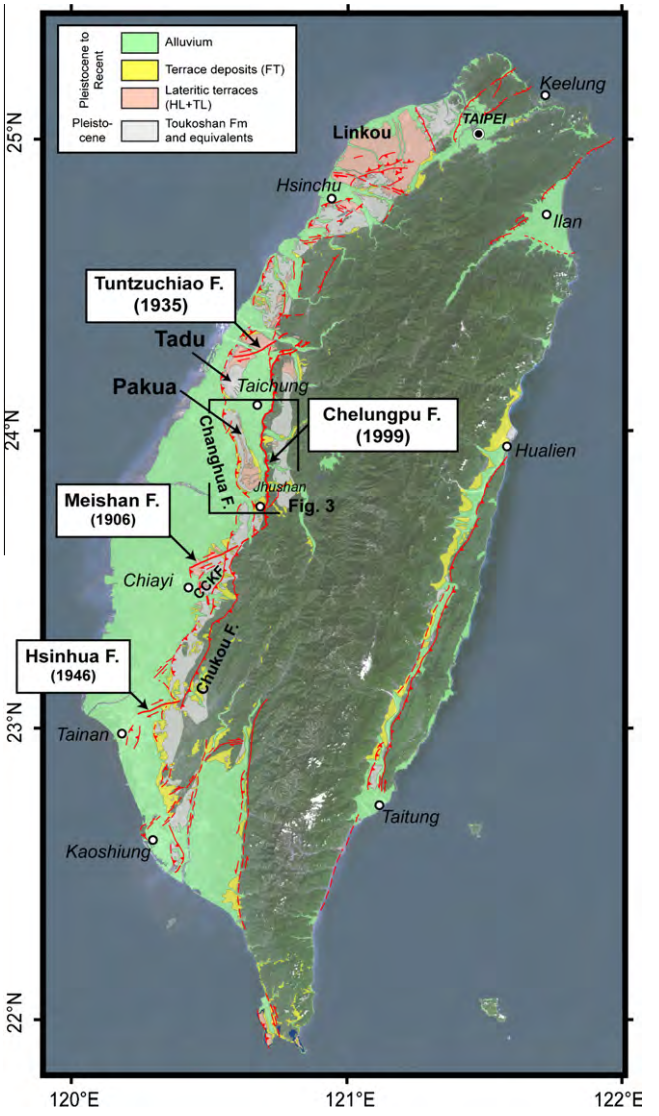

Fig. 2. Distribution of the Quaternary deposits (after Chen et al. (2000)) and main active faults (after Angelier and Chen (2002), Shyu et al. (2005), Ota et al. (2006, 2009), Chen et al. (2007a,b), Yue et al. (2009)) mapped over a mosaic of SPOT images (©CNES/CSRSR 2011).

Sea plate is subducting toward the north beneath the Eurasian plate whereas it overrides the likely oceanic crust of the South China Sea along the Manila trench. Since roughly 6 Ma, Taiwan has been experiencing the oblique convergence between the Eurasian and Philippine Sea plates (Suppe, 1981; Angelier, 1986), which still is ongoing at a rate of roughly 82 mm/year in a NW–SE direction (Yu et al., 1997; Sella et al., 2002). Under this tectonic plate configuration, the Longitudinal Valley Fault in eastern Taiwan represents the major on-land plate suture between Eurasian and Philippine Sea plates, and the Western Foothills correspond to the deformation front of the orogenic wedge (Fig. 1). The Western Foothills is characterized by a series of sub-parallel, west-verging thrusts, resulting from the westward propagation of the mountain fronts since the Pliocene (Lee et al., 1996). This region also consists of numerous active faults (Figs. 1 and 2) with a significant part of the Taiwanese population, who is thus particularly exposed to seismic hazards.

Since the last century, four destructive or devastating earthquakes struck the Western Foothills region (Fig. 1). Among them, the 1935 Hsinchu–Taichung earthquake (M 7.3, focal depth 5 km) caused the greatest losses of the twentieth century (Ng et al., 2009) until the disastrous effects of the 1999 Chi–Chi earthquake (M_w 7.5, focal depth 8 km), which ruptured the Chelungpu Fault (Fig. 2). This large seismic event also triggered a large scientific effort for a better knowledge of the potential seismogenic sources in the whole Taiwan area (*e.g.*, Shyu et al., 2005). The fact that the coseismic rupture of the Chi–Chi earthquake was located exactly at the toe of cumulated Pleistocene geomorphic scarps marked a turning point for morpho-tectonic studies in Taiwan (Chen et al., 2002; Ota et al., 2005). During the decade following the Chi–Chi earthquake, the emergence of applications using digital elevation models (DEMs) with increasing resolution facilitated, and significantly improved, geological and geomorphic mapping of active faults (*e.g.*, Shyu et al., 2005; Lai et al., 2006; Ota et al., 2006). The advent of new techniques, such as the high-resolution airborne Light Detection and Ranging (LiDAR) data, now enables the production of DEMs with a metric resolution, allowing detecting short wave-length topographic features, even in heavily urbanized areas (Chan et al., 2007). However, even if the geomorphic features

Please cite this article in press as: Siame, L.L., et al. Pleistocene alluvial deposits dating along frontal thrust of Changhua Fault in western Taiwan: The cosmic ray exposure point of view. Journal of Asian Earth Sciences (2012), doi:10.1016/j.jseaes.2012.02.002

associated to fault activities can now be studied with a high level of resolution, the application of deformed and partially preserved alluvial terraces is too often hampered by the absence of well-documented numerical ages, precluding to accurately determining fault slip rates (*e.g.*, Chen et al., 2004; Ota et al., 2006; Chen et al., 2007a,b).

3. Alluvial terraces in Western Foothills of Taiwan

3.1. General characteristics

In the Western Foothills of Taiwan, the fluvial deposits are generally differentiated into three groups, from old to young: lateritic highlands (LHs), lateritic fluvial terraces (LTs) and non-lateritic fluvial terraces (FTs). Regarding the term lateritic, it must be underlined that the red soils covering the gravels of the oldest terraces have not yet reach the true, mature stage of lateritization (Tsai et al., 2006, 2007a,b, 2010). Actually, the so-called lateritic terraces are generally characterized by a red-clayed matrix that is well-developed in the surficial part of the gravels, grading upward into 1–10 m thick soils redder than 7.5 year in the Munsell color chart (Tsai et al., 2006). Incised and stepped below the LH and LT, the FT are generally composed of unconsolidated gravel with intercalated sandy/silty lenses, poorly stratified and sorted with clasts ranging from several millimeters to several meters. Fig. 2 shows the distribution of the alluvial terraces throughout the Taiwan Island, indicating that they are mainly localized on the Western Foothills and Coastal Plain, at the toe of the mountain belt. Since they have been deformed due to the progressive, westward propagation of the frontal thrusts, those alluvial terraces provide key geomorphic markers to quantify the tectonic rates associated to active folds and faults, crucial to apprehend seismic hazards in Taiwan.

3.2. Existing chronological constraints

In Taiwan, it is particularly difficult to obtain sedimentation ages for middle Pleistocene or younger alluvial terraces. Indeed, finding material for radiocarbon or biostratigraphic dating is generally a challenge under the prevailing, highly oxidizing weathering conditions. In addition, the highly dynamic conditions of fluvial deposition enhance the probability for material recycling, particularly from one terrace to another. Nevertheless, the radiocarbon technique has been applied successfully to date geomorphic features in Taiwan, bringing Holocene to the early Pleistocene temporal constraints for studies of volcanic events (Chen et al., 2010a,b; Belousova et al., 2010), active tectonics (Liew et al., 1993; Vita-Finzi, 2000; Lee et al., 2001; Chen et al., 2001, 2003a,b, 2009; Streig et al., 2007; Hsieh and Rau, 2009; Yen et al., 2009) as well as gravitational collapse events (Hsieh and Chyi, 2010), alluvial (Hsieh and Knuepfer, 2001; Ota et al., 2002) and marine terraces (Yamaguchi and Ota, 2001; Hsieh et al., 2006). The time range of radiocarbon dating being limited at best to the last 45 kyr, terraces older than that have been dated using approaches, such as luminescence-based techniques (Wintle and Murray, 2006; Wintle, 2008; Preusser et al., 2009). In Taiwan, Optically-Stimulated Luminescence (OSL) have already provided dates for river terraces (Chen et al., 2003a,b; Simoes et al., 2007; Ota et al., 2009; Yue et al., 2009; Le Beon et al., 2010; Wu et al., 2010), in paleoseismological trenches (Chen et al., 2009) or for deposits of glacial origin preserved in the high mountainous areas (Hebenstreit and Böse, 2003; Hebenstreit et al., 2006).

Although available age controls are scarce, previous studies gave temporal benchmarks allowing addressing a general chronological framework of terrace emplacement in Western Foothills of Taiwan. Based on palynological correlations (Liew, 1988), and limited radiocarbon dating (Chen and Liu, 1991; Ota et al., 2002), the LH and LT are generally given to be older than 30 kyr. On the basis of paleomagnetic correlations, Lee et al. (1999) estimated that the LH could be as old as 900 ka. Tsai et al. (2006) studied the weathering characteristics of the red soils using the crystallinity ratio of free iron oxydes and, correlating them to dated terraces from Kikai Island in Japan (Maejima et al., 2002), they estimated an age as old as 400 ka for the LH in central Taiwan. The fluvial, non-lateritic terraces being stepped at elevations lower than those of the LH and the LT, they are generally given to be younger than 30 kyr (Chen and Liu, 1991; Sung et al., 1997; Hsieh and Knuepfer, 2001; Ota et al., 2002).

3.3. Alluvial terraces in central western Taiwan

We select the central part of the Western Foothills for deciphering timing of active tectonics in connection with the propagation of the deformation front of the Taiwan mountain belt (Fig. 2). To the west of the Chelungpu Fault, the Changhua Fault marks the present-day most advanced deformation front of the orogen (Ho, 1986; Lee et al., 1996; Delcaillau et al., 1998; Mouthereau et al., 1999). The geomorphic expression of this blind fault is dominated by the development of elongated and sigmoidal tablelands (the Tadu and Pakua tablelands), separating the Coastal Plain from the Taichung Basin (Fig. 2). To the south, the Pakua Tableland, which is about 30 km long and 5–10 km wide, comprises Quaternary terrestrial deposits that are asymmetrically folded, defining a gently dipping, 6–7 km long backlimb, and a much narrower, steeper front limb of roughly 2 km long (Simoes et al., 2007; Yue et al., 2009).

The southern part of the Pakua tableland exhibits wide, unpaired FT (deposited by the paleo-Choshui River and its tributaries) that have been abandoned while uplifted and tilted during the growth of the Pakua anticline (Fig. 3). For consistency with previous studies, we chose to name the Pakua terraces according to Tsai et al. (2006). The highest geomorphic surface in the area (LH, Pk-1) is preserved along the hinge of the Pakua anticline at roughly 440 m above the sea level (Fig. 3). The other fluvial terraces (LT, Pk-2 to Pk-6) are incised and stepped below this geomorphic surface at elevations ranging from roughly 430 m (Pk-2) to 320 m (Pk-6) above sea level (Fig. 3). South of the Pakua Tableland termination, the Choshui River is presently flowing down westwardly from the mountain front at an elevation of roughly 100 m above the sea level (Fig. 3). Below the fluvial deposits, the base rock is made of coarse conglomerate from the upper Toukoshan Formation (0.5–1 Ma; Teng, 1987; Liew, 1988), slightly inclined (<10°E), and crops out in eroded or incised cliffs, particularly along the western edge of the Pakua tableland.

On the basis of degrees of pedogenesis, Tsai et al. (2006, 2007b) established a soil chronosequence of the river terraces developed on the Pakua Tableland. Following the World Reference Base classification system (ISSS Working Group WRB, 1998), the Pk-1 pedon (highest terrace) is a Haplic Ferralsol, whereas Pk-2 to Pk-5 pedons are Haplic Acrisols, and Pk-6 pedon (lowest terrace) is a Haplic Cambisol (Tsai et al., 2007b). From the pedogenic point of view, the highest level (Pk-1) is thus, not surprisingly, the most weathered, that is, the oldest soil in the Pakua region. Based on a comparison of the weathering characteristics of the Pakua pedons, Tsai et al. (2008) estimated that the ages of the Pakua terraces should be less than 400 ka, judging from a minimum soil age of 386 ka determined using meteoric ^{10}Be dating (*e.g.*, Graly et al., 2010) of the Ultisols in Chiayi, southern Taiwan (Fig. 2). In the Tadu area, Tsai et al. (2010) estimated that the most widely spread alluvial terrace caping the tableland should be contemporaneous to the Pakua Pk-2 terrace. Within such a chronological framework, the

Please cite this article in press as: Siame, L.L., et al. Pleistocene alluvial deposits dating along frontal thrust of Changhua Fault in western Taiwan: The cosmic ray exposure point of view. Journal of Asian Earth Sciences (2012), doi:10.1016/j.jseaes.2012.02.002

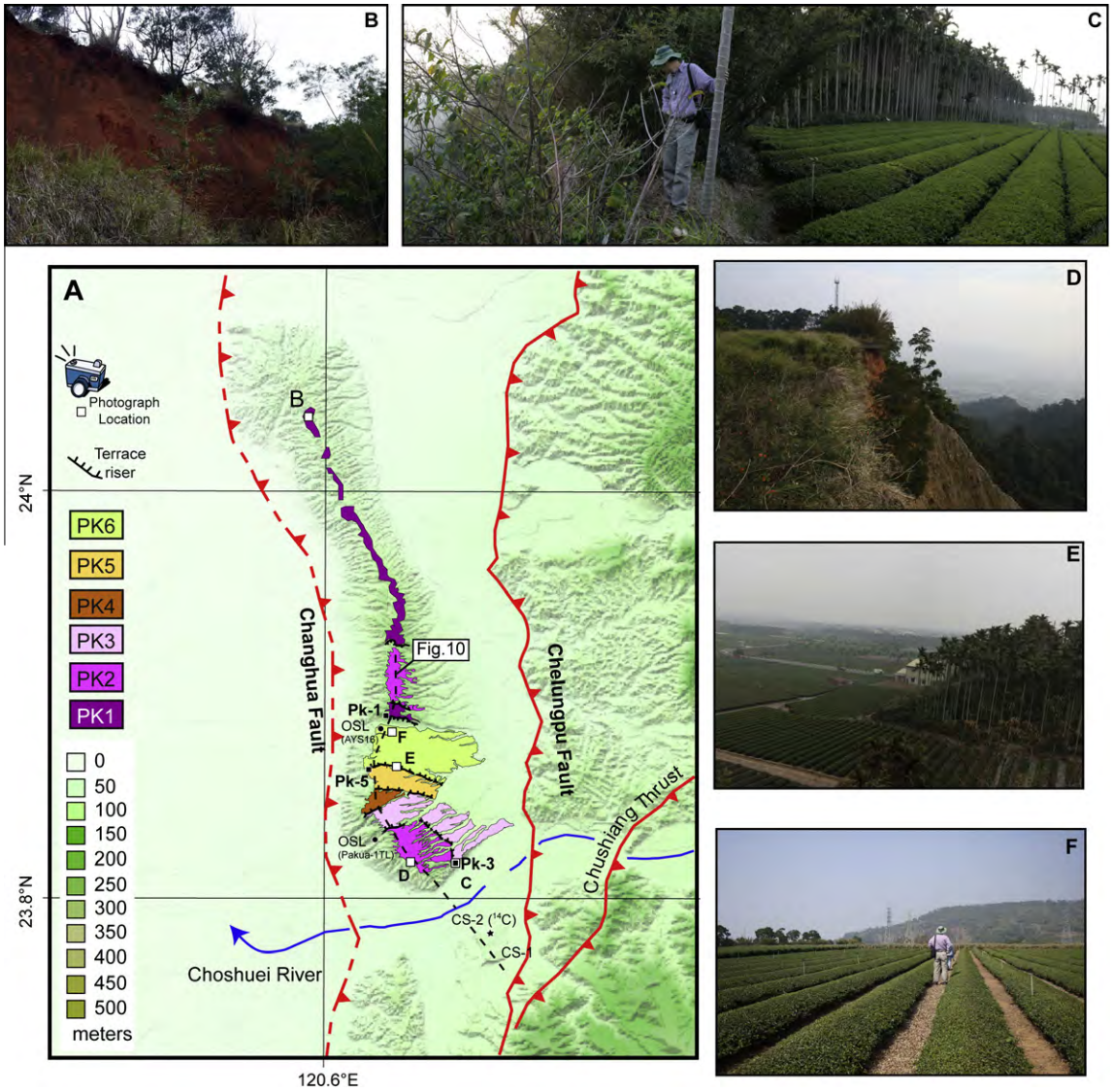

Fig. 3. (A) Geomorphic map of the Pakua Tableland locating the active faults and showing the distribution of the Quaternary lateritic terraces (LH and LT). OSL samples (black circles) are from Simoes et al. (2007). Radiocarbon-dated terrace (black star) is from Ota et al. (2002). Black squares locate the cosmogenic depth profiles analyzed in this study. Open squares locate the field photographs. (B) Red soils covering the Pk-1 terrace in the northern part of the Pakua Tableland. (C) Photograph of the terrace Pk-3 looking to the northeast. (D) Photograph of the Pk-2 border on the western edge of the Pakua Tableland. Rejuvenation of the slope is due to a landslide triggered by the 1999 Chi–Chi earthquake (old road). (E) Photograph of the Pk-5/Pk-6 terrace riser looking eastward. (F) Photograph of the Pk-6 terrace looking northward towards the Pk-1/Pk-6 riser.

deformation associated to the onset and growth of the Pakua anticline, which was in close relation with the Changhua Fault, should thus not be younger than the abandonment of the Pk-1 terrace (Delcaillau et al., 1998), that is, about 400 kyr ago.

In the same region, Simoes et al. (2007) proposed a drastically different chronological framework. Using OSL dates, they proposed that the abandonment of Pk-6 and Pk-2 terraces both occurred during the last 19 ± 4 kyr (Fig. 3). In addition, on the basis of similar tilt values, they also correlated the higher terrace Pk-1 to an alluvial terrace located further south on the left-hand side of the Choshuei River near Jhushan, which has been radiocarbon-dated by Ota et al. (2002) at 31 kyr (Fig. 3). Within such a chronological framework, their modeling of the anticline growth yielded a folding inception at about 72 kyr ago.

Thus, despite the dating efforts that have been conducted in the Pakua area, the chronological framework of the alluvial terraces remains debatable (*e.g.*, Tsai et al., 2007b, 2008; Simoes et al., 2007). To overcome this controversy, the cosmic ray exposure dating method using in situ-produced ^{10}Be along depth-profiles has been recently applied to selected alluvial deposits of the Pakua tableland (Fig. 3). However, before going into the cosmogenic-derived chronological constrains for the deformed Pakua terraces, we would like to recall the rational associated to the cosmic ray exposure dating techniques using in situ-produced ^{10}Be.

4. Cosmogenic dating of alluvial materials

To apprehend and quantify the physical processes controlling morphogenesis, one needs the establishment of detailed chronologies for environmental changes and the quantification of a large panel of surface processes. Within this general context, in situ-produced cosmogenic nuclides have literally revolutionized the way that we are able to analyze and determine the rates at which the landscapes evolve. Particularly, the techniques have been widely applied to soils and bedrock outcrops to measure their duration of exposure to cosmic rays (Bierman, 1994; Gosse and Phillips, 2001). Nowadays, measurement of the particularly low levels of

Please cite this article in press as: Siame, L.L., et al. Pleistocene alluvial deposits dating along frontal thrust of Changhua Fault in western Taiwan: The cosmic ray exposure point of view. Journal of Asian Earth Sciences (2012), doi:10.1016/j.jseaes.2012.02.002

in situ-produced cosmogenic nuclides in surface rocks and soils has become a routine, leading to the tremendous expansion of their applications in Earth Sciences. In situ-produced cosmogenic nuclides are now proved to provide chronologies of environmental change over the past few thousand to several millions of years, to quantify a wide range of weathering and sediment transport processes, and are thus widely used across a broad spectrum of Earth Science disciplines, including paleoclimatology, geomorphology and active tectonics (*e.g.*, Gosse and Phillips, 2001; Siame et al., 2006; Granger, 2006; Ivy-Ochs and Schaller, 2009).

In situ-produced cosmogenic nuclides build-up in surface rocks and soils due to the nuclear reactions induced by the interaction of secondary cosmic ray particles with target atoms in mineral lattices. Those secondary cosmic ray particles (secondary neutrons, negative muons, thermal neutrons) result from the atmospheric nuclear disintegrations when galactic cosmic rays interact with the molecules in the atmosphere. Among in situ-produced cosmogenic nuclides, ^{10}Be ($T_{1/2}$ = 1.39 Myr), ^{26}Al ($T_{1/2}$ = 0.73 Myr), and ^{36}Cl ($T_{1/2}$ = 0.30 Myr) are the most widely applied to solve geomorphic problems in siliceous (^{10}Be and ^{26}Al) and carbonated (^{36}Cl) environments. They are particularly relevant to solve geomorphic problems because their radioactive decays allow apprehending time scales spanning the last 3 Myr.

4.1. In situ-produced cosmogenic nuclides and geomorphic problems

A fundamental aspect underlying the application of in situ-produced cosmogenic nuclides to geomorphic problems is that the secondary particles are efficiently absorbed in the matter (*i.e.*, minerals in the soil profile), which limits their production to the first few meters of rock or soil below the surface. In situ-produced cosmogenic nuclides concentrations are thus proportional to the geomorphic stability of the landscape surfaces exposed to cosmic radiations. Favorable geomorphic circumstances allow using these concentrations to estimate minimum exposure ages or maximum rate of denudation (Lal, 1991; Cerling and Craig, 1994).

For all in situ-produced cosmogenic nuclides, atmospheric and geomagnetic shielding are the environmental factors that have the largest spatial effects on the surface production rates that are given normalized to sea level and high latitude (SLHL). To calculate, at a given site, the surface cosmogenic nuclide production rate, one must thus scale the SLHL production rate. The scaling scheme proposed by Stone (2000) is based on the latitude–altitude scaling factors of Lal (1991). However, Stone (2000) use the atmospheric pressure as a function of elevation, and thus take into account the physical properties of cosmic ray particle propagation in the atmosphere. The polynomials also include an improved account for the muonic component in the total cosmogenic production. Lal (1991) and Stone (2000) polynomials suppose that the cosmogenic production rate is constant through time. However, changes in the paleomagnetic field intensity have had a significant effect on cosmogenic nuclide production rates at low-latitude sites and for exposure ages higher than a few tens of ka (Masarik et al., 2001). To account for this surface production variability through time, one can either propagate a conservative uncertainty of roughly 15% (*e.g.*, Lal, 1991) or use the approach proposed by Pigati and Nifton (2004), which allows calculating time-integrated geomagnetic intensity-corrected production rates for ^{10}Be (e.g., Siame et al., 2007). Other approaches propose scaling procedures accounting for magnetic field changes (Dunai, 2001; Desilets and Zreda, 2003; Desilets et al., 2006) and solar variability (Lifton et al., 2005). Surface production rates must also be corrected for recurrent covers (snow, soils, loess), local slopes and topographic shielding due to surrounding morphologies (e.g., Dunne et al., 1999). To calculate erosion rates or exposure ages from cosmogenic nuclide concentrations one can refer to the review papers that have been recently published by Balco et al. (2008) and Dunai and Stuart (2009).

4.2. In situ-production of ^{10}Be at the surface: exposure time or denudation

Because of their efficient dissipation of their energy through nuclear reactions, the flux of secondary particles, and therefore the cosmogenic production rates, decreases exponentially with the mass of overlying material, with a characteristic attenuation length Λ (g cm^{-2}). For a flat, horizontal and unshielded surface being exposed to cosmic rays, the evolution of the cosmogenic nuclide production rate P (atoms g-mineral^{-1} year^{-1}) as a function of depth x is given by (Lal, 1991):

$$P(x) = P_0 \cdot e^{\left(-\frac{\rho x}{\Lambda}\right)} \quad (1)$$

where P_0 is the scaled surface production rate, and ρ the density of the overlying material. Stone (2000) determined SLHL production rates of 5.1 ± 0.3 atoms g^{-1} year^{-1}. However, with the recent revision of the ^{10}Be half-life (Nishiizumi et al., 2007), and since the ^{10}Be SLHL production rate published by Stone (2000) is based on measurements calibrated against non-NIST standards, it requires normalization by a factor of 1.14 ± 0.04 (Middleton et al., 1993), leading to a SLHL production rate that is correspondingly lower (4.5 ± 0.3 at/g-SiO_2/year).

For a surface exposed to cosmic rays, the cosmogenic built-up of ^{10}Be concentrations with time and depth is the result of production due to cosmic ray interaction and the losses due to denudation (ε, g cm^{-2} year^{-1}) and radioactive decay (λ, year^{-1} (Lal, 1991):

$$\frac{dN}{dt} = P_0 \cdot e^{\left(-\frac{\rho x}{\Lambda}\right)} + \varepsilon \cdot \frac{dN}{dx} - \lambda \cdot N \quad (2)$$

At the landscape surface, neutrons are the most efficient particles since they account for roughly 98% of the total ^{10}Be production (Brown et al., 1995). The 2% left are due to the muonic component of the secondary particles (Heisinger et al., 2002a,b; Braucher et al., 2003). Neutrons are very interactive particles and are thus not very penetrative with an attenuation length on the order of 150–160 g/cm^2 (Lal, 1991). Conversely, stopping and fast muons are weakly interactive but very penetrative particles with attenuation lengths on the order of 1500 and 5300 g/cm^2, respectively (Braucher et al., 2003). In other words, the relative proportion of neutrons and muons varies with depth (Fig. 4), and the muons are responsible for the rare nuclear reactions at depth once the neutrons have been attenuated. Considering the different categories of particles responsible for in situ-production of ^{10}Be, and assuming constant rates of denudation and production through time, the differential equation 2 may be solved to yield (e.g., Lal, 1991):

$$N(x,t) = N(x,0) \cdot e^{-\lambda \cdot t} + \frac{P_n}{\frac{\varepsilon \cdot \rho}{\Lambda_n} + \lambda} \cdot e^{\left(\frac{-\rho x}{\Lambda_n}\right)} \cdot \left(1 - e^{-\left(\lambda + \frac{\varepsilon \cdot \rho}{\Lambda_n}\right) \cdot t}\right) + \frac{P_{\mu s}}{\frac{\varepsilon \cdot \rho}{\Lambda_{\mu s}} + \lambda} \cdot e^{\left(\frac{-\rho x}{\Lambda_{\mu s}}\right)} \cdot \left(1 - e^{-\left(\lambda + \frac{\varepsilon \cdot \rho}{\Lambda_{\mu s}}\right) \cdot t}\right) + \frac{P_{\mu f}}{\frac{\varepsilon \cdot \rho}{\Lambda_{\mu f}} + \lambda} \cdot e^{\left(\frac{-\rho x}{\Lambda_{\mu f}}\right)} \cdot \left(1 - e^{-\left(\lambda + \frac{\varepsilon \cdot \rho}{\Lambda_{\mu f}}\right) \cdot t}\right) \quad (3)$$

where Λ_n, $\Lambda_{\mu s}$, and $\Lambda_{\mu f}$ are the effective attenuation lengths for neutrons, stopping muons and fast muons, P_n, $P_{\mu s}$, and $P_{\mu f}$, their respective surface production rates, and $N(x,0)$ is the number of cosmogenic nuclide atoms present at the initiation of the exposure episode (inheritance). Eq. (3) implies that the cosmogenic nuclide contents increase with time until they reach a steady-state balance between production and losses due to denudation and radioactive decay (Fig. 5).

Please cite this article in press as: Siame, L.L., et al. Pleistocene alluvial deposits dating along frontal thrust of Changhua Fault in western Taiwan: The cosmic ray exposure point of view. Journal of Asian Earth Sciences (2012), doi:10.1016/j.jseaes.2012.02.002

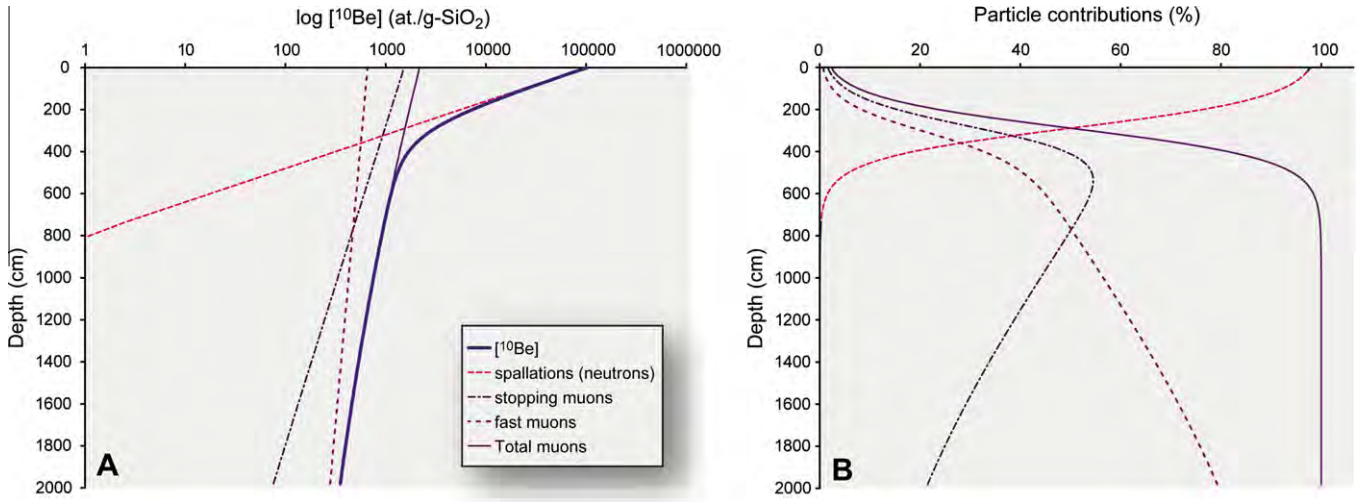

Fig. 4. Respective contribution of muons and neutrons for in situ-produced cosmogenic ^{10}Be. (A) Production as a function of depth for a surface exposure of 20 kyr and zero denudation. (B) Respective particle contributions as a function of depth. Attenuation parameters are those of Braucher et al. (2003), surface production rate is 4.5 at./g-SiO_2/an (Stone, 2000), and a material density of 2.3 g/cm^3.

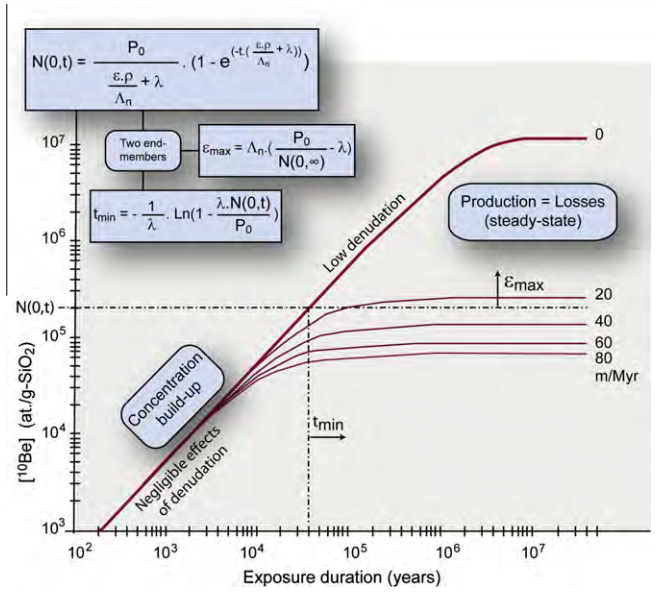

Fig. 5. In surface rocks or soils exposed to cosmic rays, cosmogenic nuclides concentration build-up with time until a steady-state balance is reached when production equals losses due to radioactive decay and denudation. Favorable geomorphic circumstances (simple exposure, negligible denudation) allow using those concentrations to calculate a minimum exposure age. Conversely, if the steady state equilibrium is reached (long time span exposure or high denudation rate) then maximum denudation rates can be calculated. Po: surface production rate, N: Concentration, ρ: density, Λ_n: neutrons attenuation length, λ radioactive decay constant, ε: denudation rate, t: time.

At the surface, if considering a single exposure scenario (with no inheritance), Eq. (3) can be simplified by neglecting the muonic terms:

$$N(0,t) = \frac{P_0}{\frac{\varepsilon\cdot\rho}{\Lambda_n}+\lambda}\cdot\left(1-e^{-\left(\frac{\varepsilon\cdot\rho}{\Lambda_n}+\lambda\right)\cdot t}\right) \quad (4)$$

where P_0 is the surface production rate, N, the ^{10}Be concentration, ρ, the density of the material, Λ_n, the attenuation length of neutrons, λ, the radioactive decay constant of the cosmogenic nuclide, ε, the denudation rate, and t, the duration of exposure (Fig. 5). It thus appears that the surface concentration is a function of both time and denudation, which makes two unknowns for one equation. On the one hand, if the exposure duration is long enough as the cosmogenic nuclide concentrations reach the steady-state equilibrium, a maximum denudation rate can be calculated (Lal, 1991). This end-member is nonetheless the basis for catchment-wide denudation determinations (von Blanckenburg et al., 2004; von Blanckenburg, 2005; Siame et al., 2010). On the other hand, to determine an exposure age from the measured surface concentrations, one must either considers that the denudation is negligible (or known by an independent method) or that the exposure duration is long enough with respect to the denudation processes (Fig. 5). In desert settings, one can have geomorphic evidences that the denudation processes have had no or very little effect on the landscape preservation and that the term ε can be neglected. In the mid-1990s, the application procedures for in situ-produced cosmogenic nuclides have been validated for relatively ideal geomorphic features for which the processes (erosion, burial...) acting on the landscape surface after their abandonment are very limited. Such favorable environmental circumstances have prompted pioneer applications in active tectonics (Bierman et al., 1995; Ritz et al., 1995; Siame et al., 1997; Van der Woerd et al., 1998). This also may be true if considering short time spans (on the order of 10^3–10^4 years) during which erosion may have had no or little effect on the preservation of the geomorphic features (Fig. 5), as revealed by the preservation of glacial striations on scoured bedrocks (*e.g.*, Siame et al., 2007). As far as these geomorphic circumstances can be demonstrated, the cosmogenic nuclide surface concentrations can be used for surface exposure dating, yielding minimum exposure durations to cosmic rays (Fig. 5). However, post-depositional processes can complicate the evolution of geomorphic surfaces and exposure ages calculated from the surface concentrations may not be representative for the actual abandonment age of the studied geomorphic features. Within this context, criteria for determining whether a surface is eroding or undergoing burial, as well as quantitative information on denudation or burial rates, may be obtained from cosmogenic nuclide depth profiles.

4.3. In situ-production of ^{10}Be along depth profiles: exposure time and denudation

Among the various techniques using in situ-produced cosmogenic nuclides, that using the measurement of ^{10}Be concentrations

Please cite this article in press as: Siame, L.L., et al. Pleistocene alluvial deposits dating along frontal thrust of Changhua Fault in western Taiwan: The cosmic ray exposure point of view. Journal of Asian Earth Sciences (2012), doi:10.1016/j.jseaes.2012.02.002

along depth profiles sampled below the surface (Brocard et al., 2003; Siame et al., 2004; Wolkowinsky and Granger, 2004; Braucher et al., 2009; Hidy et al., 2010) is one of the most promising for determining exposure scenarios for fluvial terraces (Carcaillet et al., 2009; Matsushi et al., 2006; Schmidt et al., 2011; Rixhon et al., 2011). Thanks to the refinement of the physical parameters involved in the production of in situ-produced cosmogenic nuclides (Brown et al., 1995; Heisinger et al., 2002a,b; Braucher et al., 2003), not only does this approach allow determining abandonment ages of fluvial deposits but also estimating the integrated denudation rate acting on the deposits since their abandonment, as well as the cosmogenic content of the fluvial gravels inherited from exposure prior to their deposition (Braucher et al., 2009; Hidy et al., 2010).

The depth-profile technique relies on the opposing duality of secondary neutrons and muons for in situ-production of ^{10}Be at depth. Indeed, when compared to high-energy nucleons like secondary neutrons, muons have the capacity to penetrate more deeply into rocks and the production rate of ^{10}Be varies with depth as the dominant production process progresses from nucleon spallation at the surface, to negative muon capture, and fast muon reactions at great depth (Fig. 4). This means that whereas neutron-induced production is dominant near the surface (Brown et al., 1995), reactions with muons become dominant below a few meters (Stone et al., 1998; Granger, 2006). This opposition between muonic and spallogenic particles is potentially very useful because the sensitivity to denudation decreases as the attenuation length for production increases. Used in combination along depth profiles, the concentrations measured in the upper part (usually <3 m) of the profile, dominated by the efficiently attenuated neutrons and that thus rapidly reach cosmogenic production steady-state, allow estimating the denudation rate while the concentrations measured in the lower part (>3 m) dominated by the significantly less attenuated muons allow estimating the exposure duration (Siame et al., 2004; Braucher et al., 2009; Hidy et al., 2010).

Siame et al. (2004) showed that measurement of ^{10}Be concentrations along a depth profile allows estimating both exposure time and denudation rate using a chi-square (χ^2) inversion model:

$$\chi^2 = \sum_{i=1}^{N} \frac{(N_i - N(x_i, \varepsilon, t))}{\sigma_i} \quad (5)$$

where N_i is the measured cosmogenic concentration at the depth x_i, and $C(x_i, \varepsilon, t)$ is the theoretical ^{10}Be concentrations computed using Eq. (3) with a given time-denudation (t, ε) pair. Braucher et al. (2009) have mathematically proved that for two measured ^{10}Be concentrations sampled at different depths below a surface undergoing denudation and a single exposure to cosmic rays, only one (t, ε) pair is necessary to define the system. This is true only if all the particles (neutrons, fast and stop muons) involved in the production of in situ-produced ^{10}Be are used in the model.

In the model adopted by Siame et al. (2004), the analytical uncertainties (1σ) associated to the modeled parameters were not strictly accounted for. To overcome this caveat, Braucher et al. (2009) have proposed a Monte Carlo procedure to generate randomly a large number of depth profiles within the analytical uncertainties of the measured cosmogenic concentrations, assuming that they are normally distributed. In this procedure, numerous depth profiles (at least 100) are generated by randomly selecting a concentration within the concentration ranges defined by the measured uncertainties (1σ) at each sampling depth. Then, loops on exposure time, denudation rate, integrated overall density and inheritance are performed, and for each set of parameters a chi-square value is determined. Considering all the generated depth profiles for a given set of parameters, a median value, corresponding to the median of all the chi-square values determined with the same quadruplet, is calculated. The minimum median value gives the (t, ε) pair solution.

When the measured depth profile is close to an ideal exponential decrease, and if the analytical uncertainties are better than 5%, the minimum absolute chi-square and median values converge to the same solution (Braucher et al., 2009). However, even if a unique (t, ε) solution can theoretically be found for a given profile, the measured concentrations are never exactly fitted by the model because the deposits can be affected by post-depositional processes such as bioturbation (animals or roots) or material compaction (illuviation, carbonate dissolution…). Following Bevington and Robinson (2003), one standard error of uncertainty can be circumscribed on the chi-square space for the modeled parameters where it increases by one from its lowest value (Granger, 2006). The uncertainty on the modeled parameters obtained in this way is very similar to that obtained from Monte-Carlo approaches (e.g., Braucher et al., 2009; Hidy et al., 2010). Even if such modeling of exposure scenario is very useful to provide a unique solution for the parameters controlling the cosmogenic built-up of in situ-produced ^{10}Be, it will always be necessary for the end-users considering the geological and geomorphic evidences to evaluate the model output and its significance.

5. Applications to alluvial landforms in Taiwan

5.1. Cosmogenic measurements in Taiwan

In Taiwan, the previous studies using cosmogenic nuclides published so far have been dedicated to either measuring erosion (Lee et al., 1993; Siame et al., 2010) and incision rates (Schaller et al., 2005) or constraining timing of glacial morphologies preserved in the high mountains (Carcaillet et al., 2007; Siame et al., 2007; Hebenstreit et al., 2011). Regarding rates of fluvial processes, the pioneer study by Lee et al. (1993) used the flux of meteoric ^{10}Be to estimate rates of deposition in the Taiwan Strait. In the Taroko gorges, Schaller et al. (2005) used in situ-produced ^{36}Cl exposure ages to estimate rates of river incision. More recently, Siame et al. (2010) used in situ-produced ^{10}Be to estimate rates of denudation integrated at the watershed scale in the Lanyang Valley (NE Taiwan). Regarding dating of landforms, Carcaillet et al. (2007), Siame et al. (2007) and Hebenstreit et al. (2011) used in situ-produced ^{10}Be to constraint the timing of early Holocene glacial deposits in the Nanhu Mountains (NE Taiwan). In the Western Foothills, Tsai et al. (2008) used meteoric ^{10}Be to date soils covering alluvial deposits, with a limited success and providing only minimum ages. The data presented hereafter represent more comprehensive chronological constraints for alluvial landforms in Taiwan using in situ-produced ^{10}Be.

Measuring in situ-produced cosmogenic nuclide concentrations of alluvial terraces in Taiwan is relatively challenging for two main reasons. First, at low elevations like those characterizing the Western Foothills area, surface production rates are low because of the latitudinal situation of Taiwan, centered on the Tropic of Cancer. Second, because of its geodynamic and climatic settings, characterized by frequent large earthquakes and severe typhoons triggering landslides, erosion rates are among the highest in the world and preservation of geomorphic features is difficult. In Taiwan, an additional difficulty also arises from the fact that fluvial terraces are generally covered by relatively thick soils. Determining the amount of time since their abandonment using the classical surface exposure technique is thus problematic since no surface boulders can generally be sampled. In the southern termination

Please cite this article in press as: Siame, L.L., et al. Pleistocene alluvial deposits dating along frontal thrust of Changhua Fault in western Taiwan: The cosmic ray exposure point of view. Journal of Asian Earth Sciences (2012), doi:10.1016/j.jseaes.2012.02.002

Table 1
Measured $^{10}Be/^{9}Be$ ratios and ^{10}Be concentrations used for modeling of cosmogenic depth profiles in the Pakua region. $^{10}Be/^{9}Be$ ratios were corrected for procedural blanks and calibrated against the NIST standard reference material 4325 by using an assigned value of $2.79 \pm 0.03 \times 10^{-11}$ and using a ^{10}Be half-life of $(1.387 \pm 0.012) \times 10^{6}$ year (Korschinek et al., 2010; Chmeleff et al., 2010). This standardization is equivalent to 07KNSTD within rounding error. Surface production rates are calculated following Stone (2000). Uncertainties on ^{10}Be concentrations are calculated using the standard error propagation method using the quadratic sum of the relative errors associated to the counting statistics, AMS internal error (0.5% for ASTER), and error associated to procedural blanks (Arnold et al., 2010). Thickness of samples was comprised between 3 and 5 cm. N refers to the number of counts during 3600 s of measurement.

Sample	Depth (cm)	Latitude (°N)	Elevation (m)	Shielding	Surface production rate (at./g/year)	$^{10}Be/^{9}Be$ (10^{-15})	Counts	^{10}Be concentrations (at./g)	
								Value	Error
PK-5		23.871	322	1	4.24				
PK-5, 100	100					190.21	779	109433	4031
PK-5, 130	130					127.32	134	73500	6495
PK-5, 160	160					74.84	214	46500	3350
PK-5, 220	220					40.14	359	21852	1372
PK-5, 280	280					28.85	34	13529	2569
PK-5, 370	370					22.06	68	9526	1384
PK-5, 450	450					17.89	61	9058	1461
PK-5, 500	500					20.75	73	10312	1477
PK-5, 600	600					11.11	2	4380	3887
PK-3		23.827	253	1	4.02				
PK-3, 50	50					238.38	642	161676	6502
PK-3, 100	100					145.13	305	73948	4341
PK-3, 150	150					64.38	271	36614	2392
PK-3250	250					63.32	204	34,635	2588
PK-3, 300	300					33.23	158	34,000	5279
PK-3, 570	570					25.27	130	11,886	1271
PK-3, 650	650					18.51	73	8340	1238
PK-3, 750	750					38.31	92	18,830	2158
PK1		23.895	433	1	4.61				
PK-1, 100	100					140.96	641	143,513	6872
PK-1, 250	250					131.85	783	124,982	5697
PK-1, 400	400					40.51	283	28,180	3320
PK-1, 500	500					14.82	56	8150	3663
PK-1, 600	600					17.68	75	8502	2876
PK-1, 700	700					14.55	61	6851	3132
PK-1, 800	800					10.71	36	4146	3552
Chemical blank for Pk-3 and Pk-5						2.17	14		
Chemical blank for Pk3-300 et Pk-1						6.42	5		

of the Pakua tableland (Fig. 3), measurement of in situ-produced ^{10}Be concentrations along profiles sampled below the surface was thus privileged to test the applicability of the procedure using modeling of the exponential decrease of the ^{10}Be concentrations with depth.

In this study, we used in situ-produced ^{10}Be resulting from spallation and muonic reactions on Silicon and Oxygen in quartz minerals. After sieving (fraction comprised between 1 and 0.250 mm), samples passed through magnetic separation, and non-magnetic fraction undergone selective etchings in fluorosilicic and hydrochloric acids to eliminate all mineral phases but quartz. Quartz minerals then undergone a series of selective etching in hydrofluoric acid to eliminate potential surface contamination by ^{10}Be produced in the atmosphere (e.g., Brown et al., 1991). The cleaned quartz minerals were then completely dissolved in hydrofluoric acid after addition in each sample of 100 µl of an in-house 3×10^{-3} g/g ^{9}Be carrier solution prepared from deep-mined phenakite (Merchel et al., 2008). Hydrofluoric and Perchloric fuming was used to remove fluorides and both cation and anion exchange chromatography were used to eliminate iron, aluminum, manganese and other elements. Beryllium oxide was mixed to 325-mesh niobium powder prior to measurements by Accelerator Mass Spectrometry (AMS). Measurements were performed at ASTER (Aix-en-Provence) AMS French facilities (Table 1). The ^{10}Be half-life of $(1.39 \pm 0.01) \times 10^{6}$ years used is that recently recommended by Korschinek et al. (2010) and Chmeleff et al. (2010) according to their two independent measurements.

5.2. Dating the Pakua terraces using cosmogenic depth profiles

In the southern termination of the Pakua Tableland, the terrace deposits are generally well preserved along the hinge line and the backlimb of the Pakua anticline (Fig. 3). Three sampling sites have been selected in the Pk-5, Pk-3 and Pk-1 levels in order to cover a broad time span. Profile sampling was privileged on the western edge of the hinge line where steep slopes have been rejuvenated by landslides particularly during the recent 1999 Chi–Chi earthquake (Fig. 3). On the chosen spots, the good preservation of the terrace surfaces facilitated the identification of the quartzite cobbles with depth during sampling that was conducted using climbing equipment in order to reach down 6 to 8 m depth below the surface. To establish a chronological framework for the Pakua terraces, we followed the procedure described by Braucher et al. (2009), using the measurements of cosmogenic ^{10}Be along deep depth profiles to model both the exposure time (t) and the denudation rate (ε), accounting for the ^{10}Be inheritance and the alluvial deposit density (see Section 4). To scale the surface production rates on studied sites, we used a ^{10}Be SLHL production rate of 4.5 ± 0.3 at/g-SiO_2/year, and Stone (2000) polynomials (see Section 4). To calculate the production due to muons, we adopted the approach of Balco et al. (2008), which assumes a negligible latitudinal effect on muon flux. At sampling sites, the surrounding morphologies have no impact on surface production rates, and topographic shielding does not need to be accounted for (Table 1).

Please cite this article in press as: Siame, L.L., et al. Pleistocene alluvial deposits dating along frontal thrust of Changhua Fault in western Taiwan: The cosmic ray exposure point of view. Journal of Asian Earth Sciences (2012), doi:10.1016/j.jseaes.2012.02.002

The profile sampled through the first six meters of the alluvial material capping the Pk-5 level exhibits a convincing exponential decrease of the ^{10}Be concentrations with depth, with an asymptote along the vertical abscissa indicating that the sampled alluvial material was aggraded during a single depositional event (Fig. 6). At the sampling site, the terrace is covered by a roughly 1 m thick brown soil, which was not sampled. During the modeling of the ^{10}Be concentrations with depth, none of the samples were discarded and the overall material density was treated as a free parameter within the range 1.8–2.4 g/cm^3. For this profile, the lowest chi-square solution yields an exposure of 105 ± 19 ka, which is associated with an integrated denudation rate of 3 ± 2 m/Ma and no inheritance (Fig. 6).

For the Pk-3 terrace, the profile sampled through the first 8 m of the alluvial material is characterized by the presence of a sandy lens between 2.5 and 5.7 m depth (Fig. 7). The quartzite cobbles were thus sampled at depth ranging from 0.5 (below the brown soil) and 2.5 m, as well as from 5.7 and 7.5 m depth (Fig. 7). To evaluate if this sandy lens represents a previous episode of aggradation, buried below more recent alluvial gravels, a sample of bulk sand was also taken at a depth of 3 m (Fig. 7). In such case, the concentration of the sample from the sandy lens should be significantly higher than that of the cobble sampled just above it. Though sensibly higher than the samples located at greater depths, the two concentrations measured in the sand at the top of the lens and in the cobble sampled just above it are not significantly different, leading us to consider that no significant exposure occurred before the aggradation of the top gravels. For the modeling, none of the samples were discarded and the overall material density was treated as a free parameter within the range 1.8–2.4 g/cm^3. For the Pk-3 profile, the lowest chi-square solution yields an exposure of 322 ± 25 ka, which is associated with an integrated denudation rate of 15 ± 1 m/Ma (Fig. 7). The predicted exponential decrease of the ^{10}Be concentrations with depth exhibits an asymptote towards the concentration values of the deepest samples, which are close to zero and thus bear a negligible inherited content

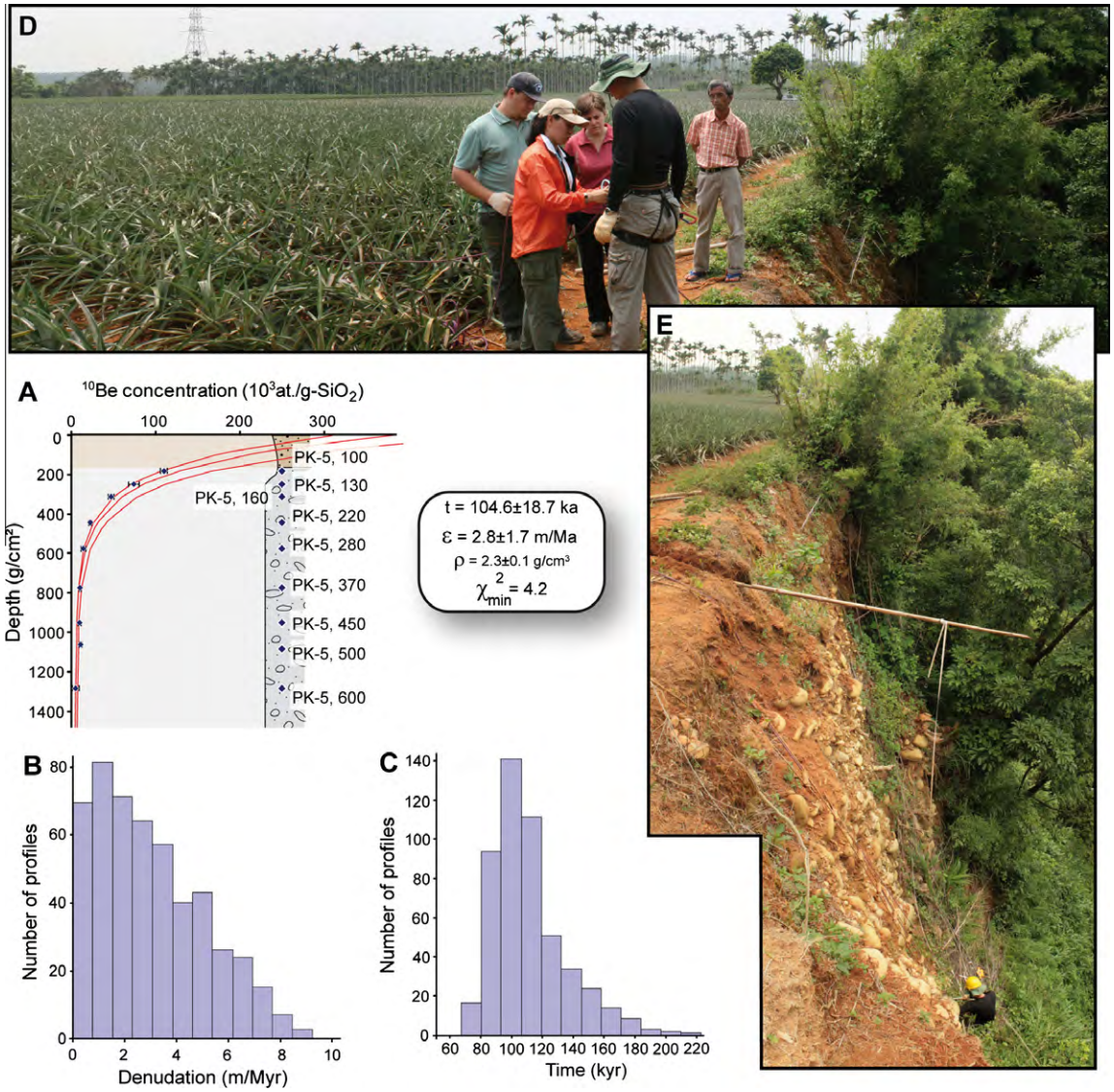

Fig. 6. (A) Depth profile within the Pk-5 alluvial terrace showing the measured in situ-produced cosmogenic ^{10}Be concentrations (Table 1) together with the result of the chi-square modeling for the exposure duration and the integrated denudation rate. (B and C) Cumulative plots of the number of profiles generated by the Monte-Carlo procedures for denudation rate and exposure duration, respectively. (D) Photograph of the Pk-5 surface at the western edge of the Pakua Tableland. (E) Photograph of the sampled section.

Please cite this article in press as: Siame, L.L., et al. Pleistocene alluvial deposits dating along frontal thrust of Changhua Fault in western Taiwan: The cosmic ray exposure point of view. Journal of Asian Earth Sciences (2012), doi:10.1016/j.jseaes.2012.02.002

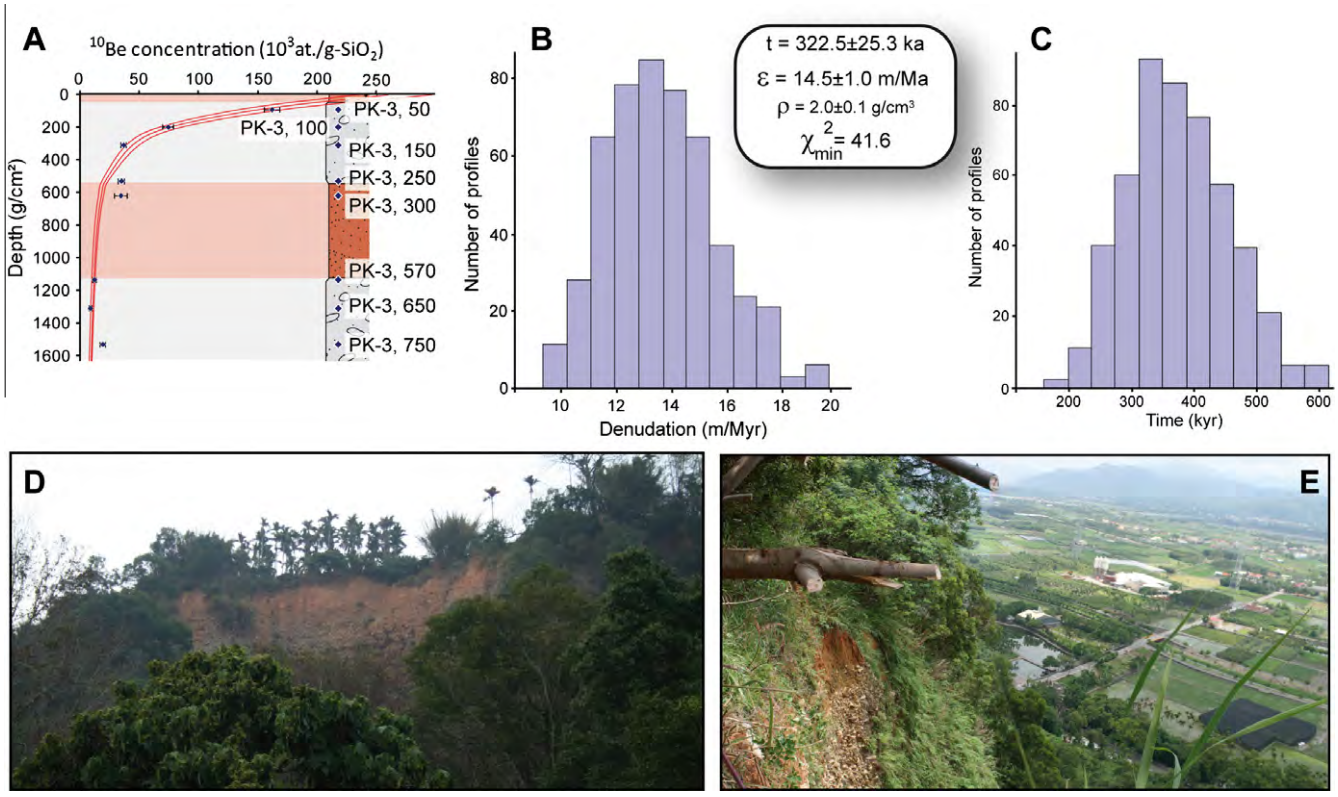

Fig. 7. (A) Depth profile within the Pk-3 alluvial terrace showing the measured in situ-produced cosmogenic ^{10}Be concentrations (Table 1) together with the result of the chi-square modeling for the exposure duration and the integrated denudation rate. (B and C) Cumulative plots of the number of profiles generated by the Monte-Carlo procedures for denudation rate and exposure duration, respectively. (C) Photograph of the Pk-3 terrace taken at the toe of the cliff looking towards the north upon the southern edge of the Pakua Tableland. (C) Photograph of the sampled section hanging high above the Choshuei River bed.

with regards to the modeled age of the Pk-3 terrace. However, though converging towards a satisfying solution, the lowest chi-square value determined for the profile is rather high and probably not as robust as that modeled for the Pk-5 terrace.

The alluvial terrace Pk-1 is covered by a thick red soil, precluding sampling cobbles within the first meters below the surface. Since the modeling of the exponential decrease of ^{10}Be concentrations with depth relies both on the neutrons close to the surface and the muons at depth (Section 4), this is a crucial issue. To overcome this, bulk soil samples were taken from the upper 4 m, whereas quartzite cobbles were sampled within the alluvial material (Fig. 8). From 8 kg of soils, roughly 15 g of quartz grains were extracted, allowing measuring ^{10}Be concentrations. Conversely to the profiles measured in the Pk-5 and Pk-3 alluvial materials, the upper part of the Pk-1 profile cannot be fitted by an exponential decrease. Indeed, the soil samples appear significantly enriched in ^{10}Be compared to the quartzite cobbles in the conglomerate at depth (Fig. 8). This situation can be interpreted as the result of vertical mixing due to bioturbation during soil development (e.g., Brown et al., 2003). Within this context, the concentrations measured in the soil samples may have reached the steady state for the production due to the secondary neutrons (Lal, 1991). If this is the case, then a steady-state denudation rate of 28 ± 2 m/Ma can be calculated from the soil samples. Such a spallogenic steady state reached during soil development does not imply that the muonic component at depth has also reached the steady state. To model the sampled depth profile, a mean concentration calculated from those measured in the soil samples has thus been assigned to the surface (Fig. 8). Using this mean concentration together with those measured at depth in the quartzite cobbles yields a lowest chi-square solution with an exposure duration of 399 ± 50 ka, an integrated denudation rate of 30 ± 2 m/Ma, and no significant inheritance as suggested by the asymptotic evolution of the measured concentrations toward values close to zero at depth (Fig. 8).

6. Discussion

6.1. Significance of the modeled denudation rates

In the Pakua area, the erosion of the uplifted landscape is usually triggered by severe storm events with a probable help from occasional large seismic events. Erosion is apparently more efficient on the western steep slopes of the tableland than on the eastern ones that are gently tilted toward the east. Indeed, on such low slopes, the evolution of the landscape is slower, except in the gullies flowing down eastwardly where mechanical erosion can locally be severe. This particular situation allowed a good preservation of the geomorphic features such as the alluvial terraces and their risers. Within such a context, the oldest terrace (Pk-1), which is also the highest of the series, is naturally the less preserved along the hinge of the Pakua anticline whereas the alluvial terraces stepped below it are better preserved at the southern tip of the Pakua Tableland (Fig. 3).

What is the geomorphic significance of the modeled denudation rates? For the Pk-3 and Pk-1 terraces, the modeled surface ^{10}Be concentrations are the same or less than for the Pk-5 terrace, which is opposite of the expected trend for increasing age. For these older terraces, higher denudation rates are thus needed. However, the denudation rates that are determined from the depth profiles have a different signification than those determined in watersheds from detrital quartz minerals (*e.g.*, Siame et al., 2010). They do not correspond to denudation rates integrated over specific drainage basins but to a local lowering of the terrace surfaces. Indeed,

Please cite this article in press as: Siame, L.L., et al. Pleistocene alluvial deposits dating along frontal thrust of Changhua Fault in western Taiwan: The cosmic ray exposure point of view. Journal of Asian Earth Sciences (2012), doi:10.1016/j.jseaes.2012.02.002

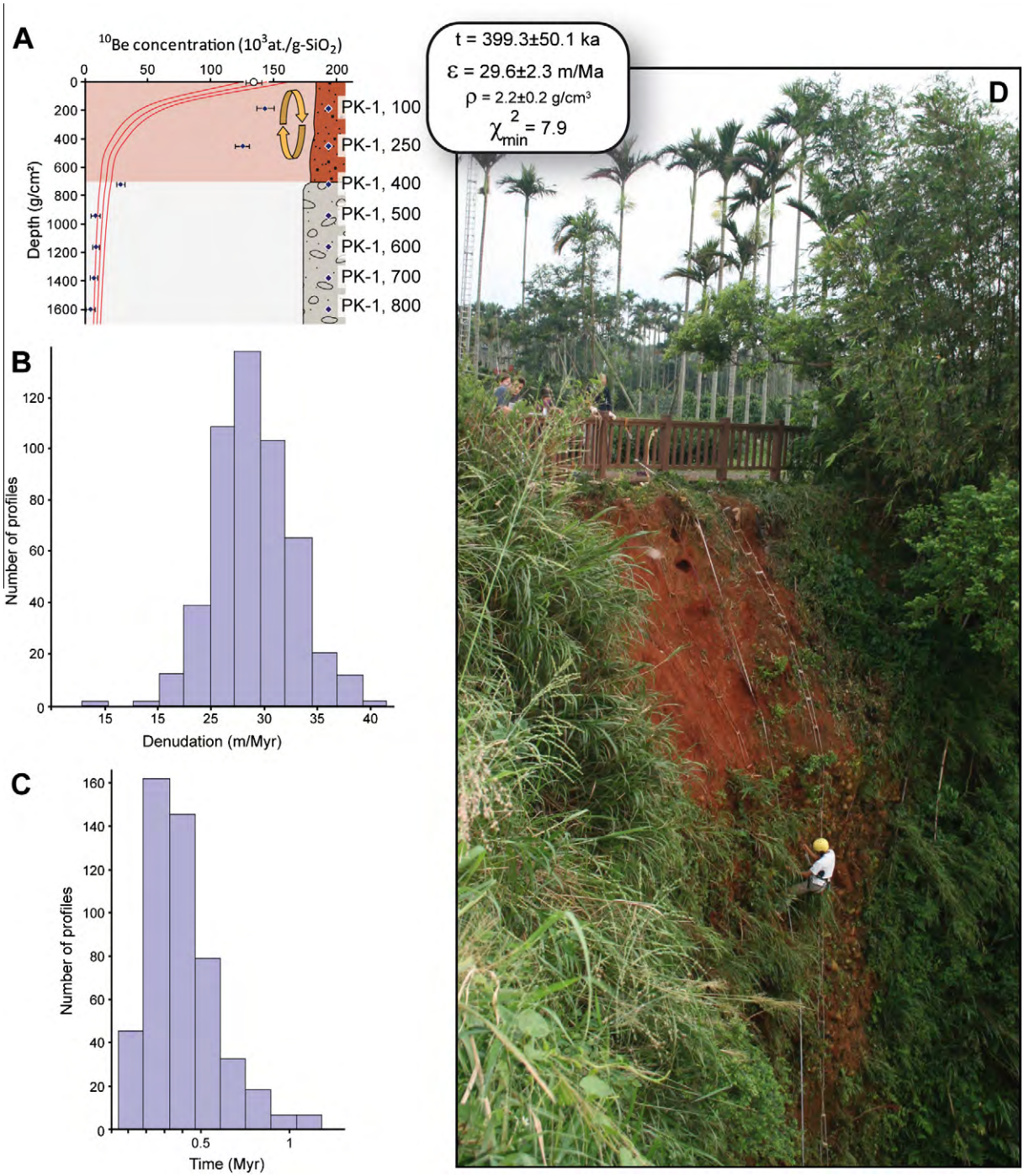

Fig. 8. (A) Depth profile within the Pk-1 alluvial terrace showing the measured in situ-produced cosmogenic ^{10}Be concentrations (Table 1) together with the result of the chi-square modeling for the exposure duration and the integrated denudation rate. The surface concentration (open circle) is the mean value of the two concentrations measured in the red soil samples (see text). (B and C) Cumulative plots of the number of profiles generated by the Monte-Carlo procedures for denudation rate and exposure duration, respectively. (D) Photograph of the sampled section.

through time, geomorphic processes, such as deflation controlled by dissolution and depletion in the upper soil horizons, through weathering and disintegration of the crystalline clasts, illuviation and compaction of the silty matrix, can be responsible for dramatic losses of matter. For the Pakua terraces, those processes resulted in the observed increase of soil weathering degree with age of the terraces (*e.g.*, Tsai et al., 2006). Within this context, a higher integrated denudation rate for the highly weathered Pk-1 terrace, and conversely a lower integrated denudation rate for the less weathered Pk-5 terrace, is not surprising. Another line of argument comes from the fact that the in situ-produced ^{10}Be concentrations measured within the uppermost meters of Pk-1 soil exhibit the characteristics of bioturbation, suggesting an evolution *en masse* of the deposits, and thus an autochthonous origin for the red soils.

The denudation rates that are determined by modeling of depth profiles correspond to rates of thickness reduction, that are averaged during the alternating climatic cycles experienced by the alluvial materials since their abandonment. According to its modeled exposure age, the youngest Pk-5 terrace has experienced only the last Interglacial/Glacial cycle whereas the older Pk-3 and Pk-1

Please cite this article in press as: Siame, L.L., et al. Pleistocene alluvial deposits dating along frontal thrust of Changhua Fault in western Taiwan: The cosmic ray exposure point of view. Journal of Asian Earth Sciences (2012), doi:10.1016/j.jseaes.2012.02.002

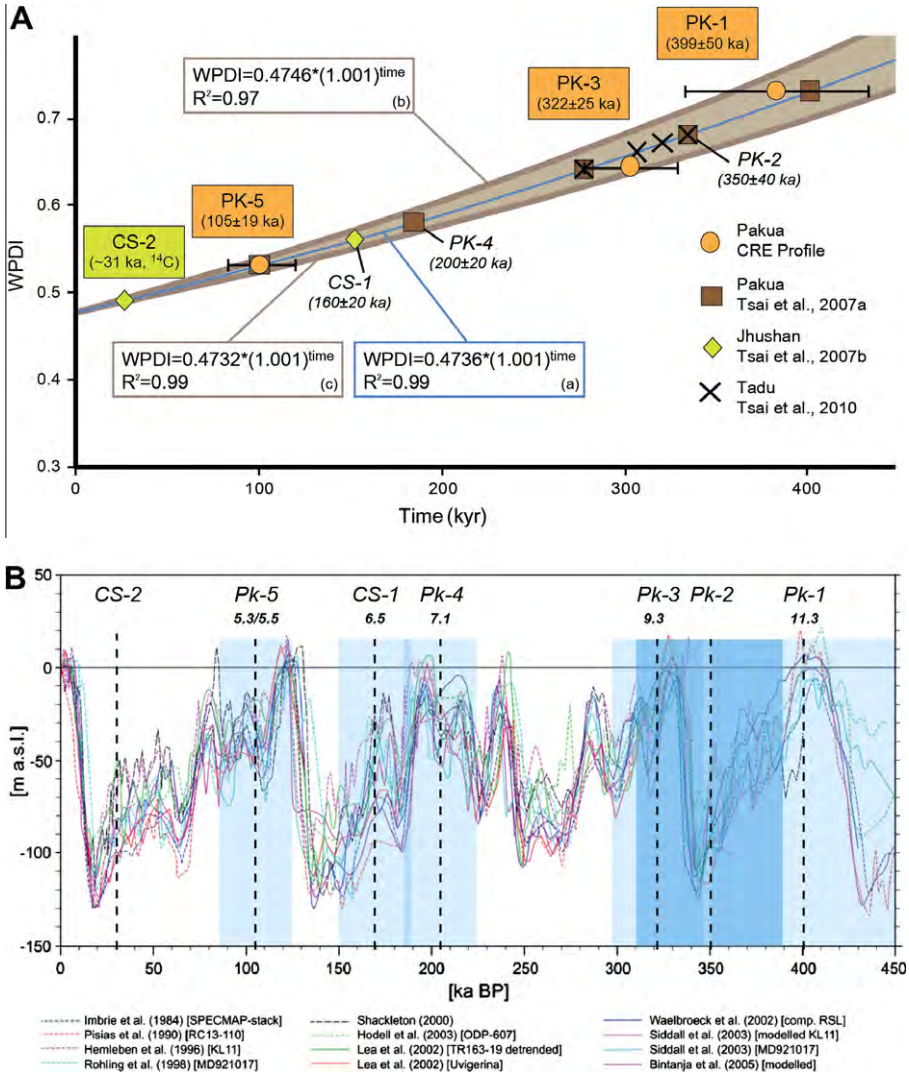

Fig. 9. (A) Regional terrace correlation using the cosmic ray exposure ages for the depth profiles sampled within Pk-5, Pk-3 and Pk-1 alluvial deposits combined with the weighted profile development indices (WPDI) determined by Tsai et al. (2007a,b). The regression curves have been obtained fitting the cosmogenic ages (and their associated uncertainties) modeled for Pk-5, Pk-3 and Pk-1 deposits with the WPDI values determined by Tsai et al. (2007a,b). The terrace CS-2, radiocarbon-dated by Ota et al. (2002), is also integrated in the regression. The thin blue line corresponds to the regression relationship using the average age values. Thick brown lines correspond to the regression relationships obtained using minimum and maximum age values (model uncertainties). Numbers in italic refer to the terrace ages determined using the correlation between WPDI and time. It is worth noting that if the regression established here is fine for data interpolation, it however does not conform to the behavior of soil development and may fail extrapolating toward both ends. B. Selected sea level curves for the last 3–4 glacial cycles (modified after Capputo, 2007), showing the possible correlations between the terrace abandonment periods and major Marine Isotope Stages. The lower and upper bounds of Pk-5 age estimate may be correlated with MIS 5.3 and 5.5, respectively. Pk-4 may be correlated with MIS 7.3, whereas CS-1 may be correlated with MIS 6.5. Given the uncertainties on the abandonment ages of Pk-4 and CS-1, an alternative interpretation would be to correlate both to MIS 7.1. For the older Pk-3 to Pk-1 terraces, the correlation is even more speculative and one possible interpretation would be to correlate PK-3 to MIS 9.3, Pk-1 to MIS 11.3 and Pk-2 to some intermediate MIS.

terraces have experienced 3–4 alternations of warm/cold climatic periods. For each terrace, the total thickness reduction can be estimated both considering the denudation rate and exposure duration determined from the modeling: 0.3 ± 0.2 m (Pk-5), 4.8 ± 0.5 m (Pk-3), and 12.0 ± 1.7 m (Pk-1). Although, the denudation rates modeled for the older terraces may appear high, they are interestingly consistent with the range of values that have been determined for alluvial material in South of France for terraces older than several hundreds of thousand years (Brocard et al., 2003; Siame et al., 2004). This reinforces the idea that the terrace thickness reduction reflects the evolution of the alluvial material during successive glacial cycles, independently of the present-day climatic regime. Such thickness reduction affecting the alluvial material as a whole, it does not have a strong impact on the geomorphic preservation of broad features like alluvial terraces, their surface being transposed in the landscape.

6.2. Significance of the modeled exposure ages

From the modeling of the Pakua profiles, it appears that the emplacement and abandonment of the alluvial terraces span the last 450 ka, in agreement with geological constraints (Delcaillau et al., 1998) and pedogenic characteristics (Tsai et al., 2006). Conversely, this cosmogenic-derived chronological framework does not match with that derived by Simoes et al. (2007) from OSL dating. Taiwan being characterized by highly dynamic depositional conditions, fluvial deposits are generally transported by high concentration flows having little opportunities for daylight exposure. Partial bleaching of the mineral grains is thus a crucial issue in dating fluvial deposits of this kind with OSL (*e.g.*, Wu et al., 2010). Another argument comes from the comparison of the pedogenic characteristics of the soils covering the terrace gravels. In their study, Simoes et al. (2007) correlated the Pk-1

Please cite this article in press as: Siame, L.L., et al. Pleistocene alluvial deposits dating along frontal thrust of Changhua Fault in western Taiwan: The cosmic ray exposure point of view. Journal of Asian Earth Sciences (2012), doi:10.1016/j.jseaes.2012.02.002

Table 2
Geomorphic parameters associated to the alluvial terraces and the incision of the Choshuei River. Elevation values correspond to the maximum elevation for a given surface extracted from the digital elevation model (40 m-resolution) along the topographic profile (B–B') shown on Fig. 3. Apparent incision values are determined by subtracting the present-day elevation of the Choshuei River to the maximum elevation for a given terrace. Corrected incision values are calculated accounting for the elevation of the global sea level with respect to the present-day one for a given terrace (+20 m for Pk-1 to Pk-5; −50 m for Pk-6 and CS-2) (*e.g.*, Capputo, 2007). Incision rates are calculated dividing the corrected incision values by the terrace ages (bold numbers correspond to modeled cosmogenic ages, italic numbers correspond to the age determined from the correlation with the WPDI published by Tsai et al. (2007b)). Terrace CS-2 has been radiocarbon-dated by Ota et al. (2002). The amount of thickness reduction has been calculated only for the modeled cosmogenic profiles. N.A.: not available.

	Elevation (m)	Incision (m)		Age (ka)		Denudation rate (m/Ma)		Thickness reduction (m)		Incision rate (mm/year)	
		Apparent	Corrected	Value	Error	Value	Error	Value	Error	Value	Error
Pk-1	**442**	**342**	**322**	**399**	**50**	**30**	**2**	**12.0**	**1.7**	**0.8**	**0.1**
Pk-2	432	332	312	*350*	*40*	*N.A.*	*N.A.*	*N.A.*	*N.A.*	*0.9*	*0.1*
Pk-3	**400**	**300**	**280**	**322**	**25**	**15**	**1**	**4.8**	**0.5**	**0.9**	**0.1**
Pk-4	390	290	270	*200*	*20*	*N.A.*	*N.A.*	*N.A.*	*N.A.*	*1.4*	*0.1*
Pk-5	**335**	**235**	**215**	**105**	**19**	**3**	**2**	**0.3**	**0.2**	**2.1**	**0.4**
Pk-6	323	223	273	*28*	*4*	*N.A.*	*N.A.*	*N.A.*	*N.A.*	*10.1*	*1.3*
CS-2	190	90	140	31	0.3	*N.A.*	*N.A.*	*N.A.*	*N.A.*	4.5	0.0
Choshuei	100										

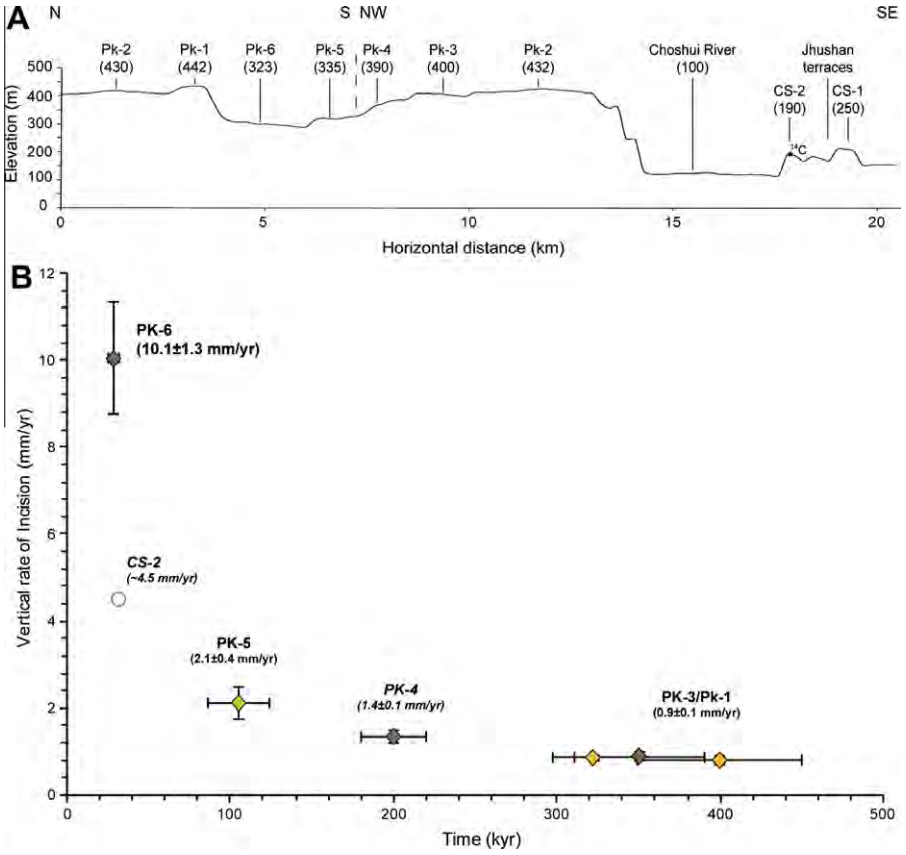

Fig. 10. (A) Topographic profile showing the stepped geometry of the alluvial terraces (located on Fig. 3). Numbers refer to the maximum elevation in meters above sea level. Vertical rate of incision experienced by the Choshuei River with respect to the present-day terrace elevations corrected for fluctuations of the sea level (Table 2).

level with a far away terrace CS-2 with radiocarbon dates at about 31 ka (Ota et al., 2002). This is debatable since the Pk-1 pedon has subsurface oxic horizons, with typical characteristics of Hapludox (Ferralsol), whereas the CS-2 pedon is much less weathered, with characteristics of Paleudult (Acrisol) (Tsai et al., 2006, 2007b). In fact, a comparison of the WPDI values determined for the terraces Pk-6 and CS-2 shows that they are most probably synchronous and implies that the Pk-6 terrace should have been abandoned 24–31 ka ago.

On the other hand, the modeled cosmogenic ages are in good agreement with those estimated using the pedogenic characteristics of the soils developed above the fluvial gravels (Tsai et al., 2006, 2008). From this observation, we thus compared the modeled cosmogenic ages with the weathering development indices (WPDI, Weighted Profile Development Index) determined by Tsai et al. (2007a,b, 2010) for pedons from the Pakua and Tadu tablelands and the alluvial terraces in Jhushan (Fig. 9). The modeled cosmogenic ages and WPDI values correlate remarkably well, fitting exponential relationships with fairly good statistics (R^2 = 0.97–0.99), allowing estimating the abandonment ages of undated terraces, with Pk-2 at 350 ± 40 ka, Pk-4 at 200 ± 20 ka, CS-1 at 160 ± 20 ka (Fig. 9). Within this framework, the terraces covering the Tadu Tableland may have been abandoned during a lag time that is synchronous to Pk-3/Pk-2; *i.e.*, 300–390 ka ago.

Please cite this article in press as: Siame, L.L., et al. Pleistocene alluvial deposits dating along frontal thrust of Changhua Fault in western Taiwan: The cosmic ray exposure point of view. Journal of Asian Earth Sciences (2012), doi:10.1016/j.jseaes.2012.02.002

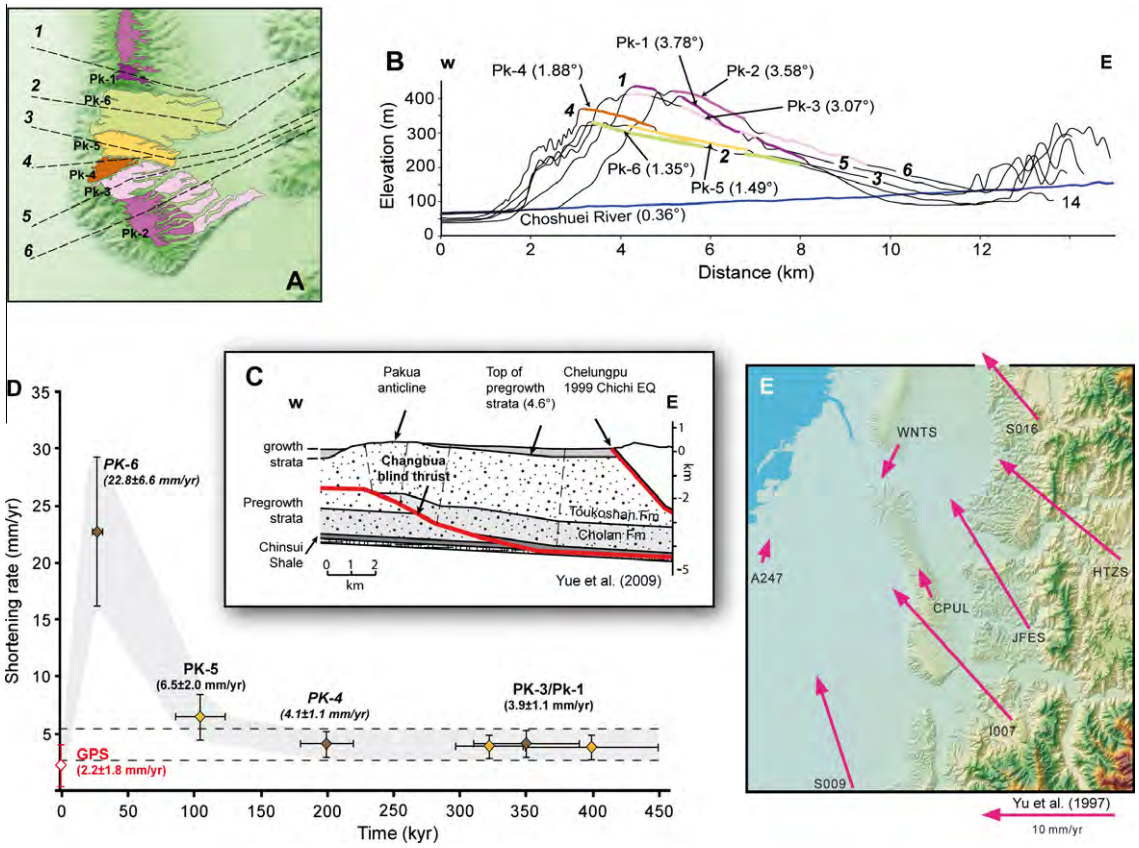

Fig. 11. (A) Close-up on the southern termination of the Pakua Tableland locating the topographic profiles shown in (B) Topographic profiles showing the terrace dip values (determined over their best preserved sections) and the present-day gradient of the Choshuei River. (C) Simplified structural interpretation of the Pakua Anticline (after Yue et al., 2009). Toukoshan–Cholan and Chinsui formations are Pleistocene and Pliocene, respectively. (D) Horizontal shortening rates associated to the Changhua Fault derived from the terrace dip values (see text and Table 3). (D) Schematic map of the GPS vectors for the stations located in the vicinity of the Pakua Tableland (after Yu et al. (1997)).

Table 3
Shortening rates associated to the Changhua Fault. Slope values correspond to the maximum slope value for a given surface, along its best-preserved section, extracted from the digital elevation model (40 m-resolution) along the topographic profiles 1–6 shown on Fig. 3. Percentages of total shortening are determined using Eq. (6). Amounts of shortening are calculated using the total input fault slip of 1686 ± 113 m determined by Yue et al. (2009). Shortening rates are calculated dividing the amounts of shortening by the terrace ages (bold numbers correspond to modeled cosmogenic ages, italic numbers correspond to the age determined from the correlation with the WPDI published by Tsai et al. (2007b).

	Slope (°)	% of total shortening	Shortening (m)		Age (ka)		Shortening rate (mm/year)	
			Value	Error	Value	Error	Value	Error
Pk-1	3.78	90	1517	393	**399**	**50**	**3.8**	**1.1**
Pk-2	3.58	86	1444	374	*350*	*40*	*4.1*	*1.2*
Pk-3	3.07	75	1257	325	**322**	**25**	**3.9**	**1.1**
Pk-4	1.88	49	821	213	*200*	*20*	*4.1*	*1.1*
Pk-5	1.49	40	678	176	**105**	**19**	**6.5**	**2.0**
Pk-6	1.35	37	627	162	*28*	*4*	*22.8*	*6.6*

The CRE ages modeled from the profiles correspond to the abandonment of the last gravel deposits, and thus benchmark the end of fluvial incision/aggradation cycles. Since the Pakua and Tadu terraces have been emplaced close to the sea shore, variations of the rivers' base level during the last 500 ka must have been related to those of the global sea level, like they were for the last 25 ka (Chen et al., 2010a,b). However, given the uncertainties associated to either the terrace abandonment ages or to the choice of a given sea level curve (*e.g.*, Capputo, 2007), it is rather challenging to assign Marine Isotope Stages (MIS). Nevertheless, from the comparison of the ages of terrace in western central Taiwan with sea-level curves, it seems that most of the terrace abandonment periods correspond to major sea level high-stands (Fig. 9).

6.3. Tectonic implications

The interaction between the growth of the Pakua anticline and incision of the Choshuei River resulted in the observed stepped fluvial terraces. During the growth of the fold, the paleo-Choshuei River flew further to the north, incising the landscape and abandoning the terraces to produce the observed series of unpaired alluvial terraces. To allow the preservation of the Pk-1 alluvial deposits from being buried below younger foreland deposits, the inception of the local uplift must thus be correlative to their abandonment. This means that some 450 ka ago, the local uplift rate due to the Changhua Fault began to be significantly higher than the subsidence rate within the Taichung Basin. If one compares the present-day elevation of the alluvial terraces to the Choshuei

Please cite this article in press as: Siame, L.L., et al. Pleistocene alluvial deposits dating along frontal thrust of Changhua Fault in western Taiwan: The cosmic ray exposure point of view. Journal of Asian Earth Sciences (2012), doi:10.1016/j.jseaes.2012.02.002

River, amounts of vertical incision can be determined (Table 2). However, these quantities correspond to apparent vertical incision since fluctuations of the sea level during the last 3–4 glacial cycles most probably controlled the behavior of the rivers flowing on the Coastal Plain. Except for the Pk-6 terrace, which corresponds to a global sea level that was roughly 50 m lower than the present-day one, the Pakua terraces seem to have been abandoned during periods of sea level high-stands that were about 15–20 m higher than today (Fig. 9). Accounting for these sea-level fluctuations, integrating the corrected amounts of vertical incision over the lifetime of the terraces implies that the paleo-Choshuei River incised below Pk-1 to Pk-3 at an average rate of 0.9 ± 0.1 mm/year (Fig. 10 and Table 2). Over a shorter time spans from Pk-4 to Pk-6 terraces, the vertical incision of the river was multiplied by a factor of ten (Fig. 10). Indeed, for the Pk-4 and Pk-5 terraces, the averaged vertical rates of incision are 1.4 ± 0.1 mm/year and 2.1 ± 0.4 mm/year, respectively, whereas it may be as high as 10.1 ± 1.3 mm/year for the Pk-6 terrace (Fig. 10 and Table 2). As a comparison, the vertical incision rate derived from the radiocarbon-dated CS-2 terrace, which is interpreted to be equivalent to Pk-6, is only on the order of 4.5 mm/year (Fig. 10 and Table 2). This underlines the fact that the increased vertical incision rate determined for the Pakua Tableland during the last 24–31 ka might well be correlative to some enhanced tectonic activity of the Changhua Fault. At the time of the abandonment of the Pk-6 terrace, the paleo-Choshuei River was defeated by the growing fold and shifted to the south where incision was much easier probably because of a much lower uplift rate south of the Changhua Fault.

From seismic reflection profiles, the Pakua anticline has been interpreted as a blind fault-propagation fold (Yue et al., 2005). On the basis of a pure-shear model and, in agreement with area of relief and bed-length shortening measurements, Yue et al. (2009) estimated a total ramp slip of about 1.7 km. The long backlimb of the anticline is marked by progressive limb rotations that are recorded by growth strata and terrace surfaces (Fig. 11). Considering the shear fault-bend folding theory (Suppe et al., 2004) that implies a nearly linear relationship between backlimb dip and horizontal shortening, Yue et al. (2009) proposed that:

$$S = \frac{\delta_{terrace}}{\delta_{pregrowth}} S_{pregrowth} \quad (6)$$

where the total input fault slip, $S_{pregrowth}$, is 1686 ± 113 m and the apparent dip of the uppermost reflectors of the seismic line, $\delta_{pregrowth}$, is 4.6 ± 0.1° (Fig. 11). From the terrace dip values determined along the best-preserved sections, amounts of shortening can thus be estimated from the relationship given by Eq. (6) (Table 3). Combining these shortening quantities with the ages determined for the Pakua terraces allows estimating shortening rates associated with the Changhua Fault (Fig. 11). Based on its dip value, the terrace Pk-1 has recorded 90% of the total input fault slip of 1686 ± 113 m determined by Yue et al. (2009). This is in good agreement with the fact the abandonment of the oldest alluvial terrace must shortly post-date the deformation inception. At the time of Pk-4 abandonment, roughly half of the total amount of shortening was already accommodated (Table 3). Afterward, the second half has thus been accommodated at an accelerating rate, and particularly during the last 31 ka (Table 3). The fact that the Pk-5 terrace is tilted only slightly more than the much younger Pk-6 terrace provides evidences for an increase of a factor of 4 in tilting rate, and thus in shortening rate (Table 3). Indeed, the shortening rates averaged from the amount of shortening cumulated during the lifetime of the alluvial terraces Pk-1 to Pk-4 remained constant at a lower rate of 4 ± 1 mm/year (Fig. 11 and Table 3). The amounts of shortening cumulated during the lifetime of the Pk-5 and Pk-6 terraces imply higher shortening rates on the order of 7 ± 2 mm/year and 23 ± 7 mm/year, respectively (Fig. 11 and Table 3).

The implications of these results are two-fold. First, the average shortening rate determined over a few hundred thousand years (3–5 mm/year) is comparable to the GPS horizontal velocities determined by Yu et al. (1997) in the vicinity of the Changhua Fault (Fig. 11). This underlines that the present-day deformation rates determined along the most frontal thrust of the Taiwan mountain belt might well be representative for the transient accumulation of elastic strain. On the other hand, as far as the age of the Pk-6 terrace is correctly estimated, the shortening rate determined over the last 31 ka (16–30 mm/year) suggests that the slip on the Changhua Fault has been accelerating to reach nearly 20–30% of the convergence rate between the Eurasian and the Philippine Sea plates (e.g., Simoes et al., 2007; Yue et al., 2009). If so, the much lower rate from the present-day GPS velocities implies a significant slip deficit, thus an ongoing strain accumulation on the Changhua Fault, which certainly deserves attention in term of seismic hazards. Alternatively, this important difference between the deformation rates determined on the middle term (30 ka) and those determined on the short (geodesy) and long (450 ka) terms might be a piece of evidence that the Changhua Fault may have experienced a series of strong earthquakes, close together in time during the last 30 ka, following a seismogenic clustering fashion.

7. Conclusions

Determining well-constrained chronological framework for landscape development in context of active tectonics is a crucial issue. Not only does this chronological framework should allow determining the ages of deformed geomorphic markers but it also should open the temporal window over time spans long enough to allow apprehending evolution and possible fluctuation in the rates of active tectonics. In this paper, we presented how the cosmogenic dating method (in situ-produced ^{10}Be) can be used to constraint the chronological framework of alluvial deposits over a Pleistocene time scale. Thanks to a comparison of our cosmogenic-derived ages with existing data such as pedogenic characteristics of the alluvial deposits, we provide a consistent regional chronological framework, spanning the last 450 ka, for the Pakua–Tadu area along the Changhua Fault, one of the most active frontal thrusts of the Taiwan mountain belt. The obtained newly revised chronological constraints allow discussing terrace abandonment ages in relation with major sea level high-stands. More importantly, those data open an interesting perspective for terrace correlation in Taiwan through the combination of cosmogenic depth profiles with pedogenic analyses. Another pathway to follow will be to systematically combine deep cosmogenic depth profiles with OSL sampling, in order to better understand the possible age discrepancies between the two techniques, and better tackle the depositional, denudation and exposure scenarios experienced by the deformed alluvial deposits.

From the point of view of active tectonics in Taiwan, the comparison of the current geodetic-derived loading rates with the shortening rates derived from our cosmogenic chronological framework provide evidences that the shortening rate absorbed by the Changhua Fault was not constant over the last 450 ka, with an acceleration commencing roughly 200 ka ago to reach a significant proportion of the convergence rate circa 30 ka. In connection with the westward propagation of the deformation front, this evolution might well be symptomatic for the maturation of the Changhua Fault during a recent period of high activity, which thus represents a serious seismic source of hazards for this populated region of western central Taiwan. At the scale of the Taiwan orogen, this observation also reinforces the idea that the deformation tend to localize on

Please cite this article in press as: Siame, L.L., et al. Pleistocene alluvial deposits dating along frontal thrust of Changhua Fault in western Taiwan: The cosmic ray exposure point of view. Journal of Asian Earth Sciences (2012), doi:10.1016/j.jseaes.2012.02.002

a few structures and that the plate convergence should be partitioned over a limited number of major fault zones accommodating fractions of the total plate velocities.

Acknowledgments

The ^{10}Be measurements were performed at the ASTER AMS national facility (CEREGE, Aix en Provence) that is supported by the INSU/CNRS, the French Ministry of Research and Higher Education, IRD and CEA. We thank F. Chauvet, M. Arnold, K. Keddadouche and G. Aumaître for their help during chemistry and measurements at CEREGE. We also thank H. Tsai for his revision of our submitted manuscript, as well as another anonymous reviewer. We also acknowledge the Taiwanese students from Academia Sinica, and National Taiwan University for their helpful climbing skills during sampling. This work was supported by the Agence Nationale pour la Recherche through the ACTS-Taiwan (Active Tectonics and Seismic Hazard in Taiwan) project. Funding of Dr. Chen R.-F.'s post-doc position was made possible thanks to Academia Sinica of Taiwan, and National Science Council of Taiwan (Grants: NSC 94-2811-M-001-008, NSC 94-2811-M-001-060, NSC 95-2119-M-001-057). We also acknowledge the BFT (Bureau Français de Taipei) and the BRT (Bureau de Représentation de Taipei en France) for their constant help.

References

Angelier, J., 1986. Geodynamics of Eurasia–Philippine sea plate boundary: preface. Tectonophysics 125, IX–X.

Angelier, J., Chen, R.-F., 2002. Empirical mathematical analysis of longitudinal river profiles reveals tectonic uplift and folding: a case in Taiwan. Comptes Rendus Geosciences 334, 1103–1111.

Angelier, J., Chu, H.T., Lee, J.C., Hu, J.C., 2000. Active faulting and earthquake risk: the Chihshang Fault case, Taiwan. Journal of Geodynamics 29, 151–185.

Angelier, J., Chang, T.Y., Hu, J.-C., Chang, C.P., Siame, L., Lee, J.C., Deffontaines, B., Chu, H.T., Lu, C.Y., 2009. Does extrusion occurs at both tips of the Taiwan collision belt? Insights from active deformation studies in the Ilan Plain and Pingtung Plain regions. Tectonophysics 466, 356–376.

Arnold, M., Merchel, S., Bourlès, D.L., Braucher, R., Benedetti, L., Finkel, R.C., Aumaître, G., Gottdang, A., Klein, M., 2010. The French accelerator mass spectrometry facility ASTER: improved performance and developments. Nuclear Instruments and Methods in Physics Research Section B: Beam Interactions with Materials and Atoms 268, 1954–1959.

Avouac, J.-P., Peltzer, G., 1993. Active tectonics in Southern Xinjiang, China. Journal of Geophysical Research 98 (B12), 21773–21807.

Balco, G., Stone, J.O., Lifton, N.A., Dunai, T.J., 2008. A complete and easily accessible means of calculating surface exposure ages or erosion rates from ^{10}Be and ^{26}Al measurements. Quaternary Geochronology 3 (3), 174–195.

Belousova, A., Belousova, M., Chen, C.-H., Zellmer, G.F., 2010. Deposits, character and timing of recent eruptions and gravitational collapses in the Tatun Volcanic Group, Northern Taiwan: hazard-related issues. Journal of Volcanology and Geothermal Research 191 (3–4), 205–221.

Bendick, R., Bilham, R., Freymueller, J., Larson, K., Yin, G., 2000. Geodetic evidence for a low slip rate on the Altyn Tagh fault system. Nature 404, 69–72.

Bevington, P.R., Robinson, D.K., 2003. Data Reduction and Error Analysis for the Physical Sciences. McGraw-Hill, 320 p.

Bierman, P.R., 1994. Using in situ produced cosmogenic isotopes to estimate rates of landscape evolution: a review from the geomorphic perspective. Journal of Geophysical Research 99 (B7), 13885–13896.

Bierman, P.R., Gillespie, A.R., Caffee, M.W., 1995. Cosmogenic ages for earthquakes recurrence intervals and debris flow fan deposition, Owen valley, California. Science 270, 447–450.

Braucher, R., Brown, E.T., Bourlès, D.L., Colin, F., 2003. In situ produced ^{10}Be measurements at great depths: implications for production rates by fast muons. Earth and Planetary Science Letters 211, 251–258.

Braucher, R., Del Castillo, P., Siame, L., Hidy, A.J., Bourlès, D.L., 2009. Determination of both exposure time and denudation rate from an in situ-produced ^{10}Be depth profile: a mathematical proof of uniqueness. Model sensitivity and applications to natural cases. Quaternary Geochronology 4, 56–67.

Bridgland, D., Westaway, R., 2008. Climatically controlled river terrace staircases: a worldwide quaternary phenomenon. Geomorphology 98, 285–315.

Brocard, G.Y., van der Beek, P.A., Bourlès, D.L., Siame, L.L., Mugnier, J.-L., 2003. Long-term fluvial incision rates and postglacial river relaxation time in the French Western Alps from ^{10}Be dating of alluvial terraces with assessment of inheritance, soil development and wind ablation effects. Earth and Planetary Science Letters 209, 197–214.

Brown, E.T., Edmond, J.M., Raisbeck, G.M., Yiou, F., Kurz, M.D., Brook, E.J., 1991. Examination of surface exposure ages of Antarctic moraines using in situ produced ^{10}Be and ^{26}Al. Geochimica et Cosmochimica Acta 55, 2269–2283.

Brown, E.T., Bourlès, D.L., Colin, F., Raisbeck, G.M., Yiou, F., Desgarceaux, S., 1995. Evidence for muon-induced production of ^{10}Be in near surface rocks from Congo. Geophysical Research Letters 22, 703–706.

Brown, E.T., Colin, F., Bourlès, D.L., 2003. Quantitative evaluation of soil processes using in situ-produced cosmogenic nuclides. Comptes Rendus Geosciences 335 (16), 1161–1171.

Burgmann, R., Rosen, P.A., Fielding, E.J., 2000. Synthetic aperture radar interferometry to measure Earth's surface topography and its deformation. Annual Review of Earth and Planetary Science 28, 169–209.

Capputo, R., 2007. Sea-level curves: perplexities of an end-user in morphotectonic applications. Global and Planetary Change 57, 417–423.

Carcaillet, J., Siame, L.L., Chu, H.-T., Bourlès, D.L., Lu, W.-C., Angelier, J., Dussouillez, P., 2007. First cosmic ray exposure dating (in situ produced ^{10}Be) of the late pleistocene and holocene glaciation in the Nanhutashan Mountains (Taiwan). Terra Nova 19, 331–336.

Carcaillet, J., Mugnier, J.L., Koçi, R., Jouanne, F., 2009. Uplift and active tectonics of southern Albania inferred from incision of alluvial terraces. Quaternary Research 71, 465–476.

Cerling, T.E., Craig, H., 1994. Geomorphology and in-situ cosmogenic isotopes. Annual Reviews of Earth and Planetary Sciences 22, 273–317.

Chan, Y.C., Chen, Y.G., Shih, T.Y., Huang, C., 2007. Characterizing the Hsincheng active fault in northern Taiwan using airborne LiDAR data: detailed geomorphic features and their structural implications. Journal of Asian Earth Sciences 31 (3), 303–316.

Chang, H.-S., Wu, Y.-M., Shin, T.-C., Wang, C.-Y., 2000. Relocation of the 1999 Chi–Chi Earthquake in Taiwan. Terrestrial, Atmospheric and Ocean Sciences 11 (3), 581–590.

Chen, Y.G., Liu, T.K., 1991. Radiocarbon dates of river terraces along the lower Tahanchi, northern Taiwan: their tectonic and geomorphic implications. Journal of the Geological Society of China 34, 337–347.

Chen, C.-H., Ho, H.-C., Shea, K.-S., Lo, W., Lin, W.-H., Chang, H.-C., Huang, C.-H., Lin, C.-W., Chen, G.-H., Yang, C.-N., Lee, Y.-H., 2000. Geologic Map of Taiwan, 1:500,000. Published by Central Geological Survey, Ministry of Economic Affairs.

Chen, W.-S., Lee, K.-J., Lee, L.-S., Ponti, D.J., Prentice, C., Chen, Y.-G., Chang, H.-C., Lee, Y.-H., 2001. Paleoseismology of the Chelungpu Fault during the past 1900 years. Quaternary International 115, 167–176.

Chen, Y.G., Chen, W.S., Wang, Y., Lo, P.W., Lee, J.C., Liu, T.K., 2002. Geomorphic evidence for prior earthquakes: lessons from the 1999 Chichi earthquake in central Taiwan. Geology 30 (2), 171–174.

Chen, Y.-G., Chen, Y.-W., Chen, W.S., Zhang, J.-F., Zhao, H., Zhou, L.-P., Li, S.-H., 2003a. Preliminary results of long-term slip rates of 1999 earthquake fault by luminescence and radiocarbon dating. Quaternary Science Reviews 22 (10–13), 1213–1221.

Chen, Y.-W., Chen, Y.-G., Murray, A.S., Liu, T.-K., Lai, T.-C., 2003b. Luminescence dating of neotectonic activity on the southwestern coastal plain, Taiwan. Quaternary Science Reviews 22 (10–13), 1223–1229.

Chen, Y.G., Shyu, J.B.H., Ota, Y., Chen, W.H., Hu, J.C., Tsai, B.W., Wang, Y., 2004. Active structures as deduced from geomorphic features: a case in Hsinchu Area, northwestern Taiwan. Quaternary International 115–116, 189–199.

Chen, W.S., Yang, C.-C., Yen, I.-C., Lee, S.-J., Lee, K.-J., Yang, H.-C., Chang, H.-C., Ota, Y., Lin, C.-W., Lin, W.-H., Shih, T.-S., Lu, S.-T., 2007a. Late Holocene paleoseismology of the southern part of the Chelunpgu fault in Central Taiwan: evidence from Chushan excavation site. Bulletin of the Seismological Society of America 91 (1), 1–13.

Chen, Y.G., Hung, J.H., Lai, K.Y., Lin, Y.N.N., Wilcox, T., Mueller, K., 2007b. River terrace development in response to folding above active wedge thrusts in Houli, Central Taiwan. Journal of Asian Earth Sciences, Earthquake Geology and Hazards in Taiwan 31 (3), 240–250.

Chen, Y.-G., Chen, Y.-W., Chen, W.-S., Lee, K.-J., Lee, L.-S., Lu, S.-T., Lee, Y.-H., Watanuki, T., Lin, Y.-N., 2009. Optical dating of a sedimentary sequence in a trenching site on the source fault of the 1999 Chi–Chi earthquake, Taiwan. Quaternary International 199, 25–33.

Chen, C.-H., Burr, G.S., Lin, S.-B., 2010a. Time of near Holocene volcanic eruption in the Tatun Volcano Group, Northern Taiwan: evidence from AMS radiocarbon dating of charcoal ash from sediments of the Sungshan Formation in Taipei Basin. Terrestrial, Atmospheric and Ocean Sciences 21 (3), 611–614.

Chen, H.W., Lee, T.Y., Wu, L.C., 2010b. High-resolution sequence stratigraphic analysis of Late Quaternary deposits of the Changhua Coastal Plain in the frontal arc-continent collision belt of central Taiwan. Journal of Asian Earth Sciences 39, 192–213.

Chmeleff, J., von Blanckenburg, F., Kossert, K., Jakob, D., 2010. Determination of the ^{10}Be half-life by multicollector ICP-MS and liquid scintillation counting. Nuclear Instruments & Methods in Physics Research Section B 268, 192–199.

Chuang, R.Y., Johnson, K.M., 2011. Reconciling geologic and geodetic model fault slip-rate discrepancies in Southern California: consideration of nonsteady mantle flow and lower crustal fault creep. Geology 39 (7), 627–630.

Dawson, T.E., McGill, S.F., Rockwell, T.K., 2003. Irregular recurrence of paleoearthquakes along the central Garlock fault near El Paso Peaks, California. Journal of Geophysical Research 108 (B7), 2356.

Delcaillau, B., Deffontaines, B., Floissac, L., Angelier, J., Deramond, J., Souquet, P., Chu, H.T., Lee, J.F., 1998. Morphotectonic evidence from lateral propagation of an active frontal fold: Pakuashan anticline, foothills of Taiwan. Geomorphology 24 (4), 263–290.

DeMets, C., Gordon, R.G., Argus, D.F., Stein, S., 1990. Current plate motions. Geophysical Journal International 101, 425–478.
DeMets, C., Gordon, R.G., Argus, D.F., Stein, S., 1994. Effect of recent revisions to the geomagnetic reversal time scale on estimates of current plate motions. Geophysical Research Letters 21, 2191–2194.
DeMets, C., Gordon, R.G., Argus, D.F., 2010. Geologically recent plate motions. Geophysical Journal International 181, 1–80.
Desilets, D., Zreda, M., 2003. Spatial and temporal distribution of secondary cosmic-ray nucleon intensities and applications to in situ cosmogenic dating. Earth and Planetary Science Letters 206 (1-2), 21–42.
Desilets, D., Zreda, M., Prabu, T., 2006. Extended scaling factors for in situ cosmogenic nuclides: new measurements at low latitude. Earth and Planetary Science Letters 246 (3–4), 265–276.
Dixon, T.H., Norabuena, E., Hataling, L., 2002. Paleoseismology and Global Positionning System: earthquake cycle effects and geodetic versus geologic fault slip rates in the Eastern California shear zone. Geology 31 (1), 55–58.
Dunai, T.J., 2001. Influence of secular variation of the geomagnetic field on production rates of in-situ produced cosmogenic nuclides. Earth and Planetary Science Letters 193, 197–212.
Dunai, T.J., Stuart, F.M., 2009. Reporting of cosmogenic nuclide data for exposure age and erosion rate determinations. Quaternary Geochronology 4 (6), 437–440.
Dunne, J., Elmore, D., Muzikar, P., 1999. Scaling factors for the rates of production of cosmogenic nuclides for geometric shielding and attenuation at depth on sloped surfaces. Geomorphology 27 (1–2), 3–12.
Fay, N.P., Humphreys, E.D., 2005. Fault slip rates, effects of elastic heterogeneity on geodetic data, and the strength of the lower crust in the Salton Trough region, southern California. Journal of Geophysical Research 110, B09401.
Friedrich, A.M., Wernicke, B.P., Niemi, N.A., Bennett, R.A., Davis, J.L., 2003. Comparison of geodetic and geologic data from the Wasatch region, Utah, and implications for the spectral character of Earth deformation at periods of 10 to 10 million years. Journal of Geophysical Research 108 (B4), 2199. doi:10.1029/2001JB000682.
Gosse, J.C., Phillips, F.M., 2001. Terrestrial in situ cosmogenic nuclides: theory and application. Quaternary Science Reviews 20, 1475–1560.
Graly, J.A., Bierman, P.R., Reusser, L.J., Pavich, M.J., 2010. Meteoric ^{10}Be in soil profiles – a global meta-analysis. Geochimica et Cosmochimica Acta 74, 6814–6829.
Granger, D.E., 2006. A review of burial dating methods using ^{10}Be and ^{26}Al: in situ produced cosmogenic nuclides and quantification of geological processes. Geological Society of America Special Paper 415, 1–16.
Grant, L.B., Sieh, K., 1994. Paleoseismic evidence of clustered earthquakes on the San Andreas fault in the Carrizo Plain, California. Journal of Geophysical Research 99, 6819–6841.
Hebenstreit, R., Böse, M., 2003. Geomorphological evidence for a Late Pleistocene glaciation in the high mountains of Taiwan dated with age estimates by optically stimulated luminescence (OSL). Zeitschrift für Geomorphologie NF Supplementband 130, 31–49.
Hebenstreit, R., Böse, M., Murray, A., 2006. Late Pleistocene and Early Holocene glaciations in Taiwanese mountains. Quaternary International 147 (1), 70–75.
Hebenstreit, R., Ivy-Ochs, S., Kubik, P.W., Schlüchter, C., Böse, M., 2011. Lateglacial and early Holocene surface exposure ages of glacial boulders in the Taiwanese high mountain range. Quaternary Science Reviews 30 (3–4), 298–311.
Heisinger, B., Lal, D., Jull, A.J.T., Kubik, P., Ivy-Ochs, S., Knie, K., Nolte, E., 2002a. Production of selected cosmogenic radionuclides by muons: 2. Capture of negative muons. Earth and Planetary Science Letters 200, 357–369.
Heisinger, B., Lal, D., Jull, A.J.T., Kubik, P., Ivy-Ochs, S., Neumaier, S., Knie, K., Lazarev, V., Nolte, E., 2002b. Production of selected cosmogenic radionuclides by muons: 1. Fast muons. Earth and Planetary Science Letters 200, 345–355.
Hidy, A.J., Gosse, J.C., Pederson, J.L., Mattern, J.P., Finkel, R.C., 2010. A geologically constrained Monte Carlo approach to modeling exposure ages from profiles of cosmogenic nuclides: an example from Lees Ferry, Arizona. Geochemistry Geophysics Geosystems 11, Q0AA10.
Ho, C.S., 1986. A synthesis of geological evolution of Taiwan. Tectonophysics 125, 1–16.
Holt, W.E., Chamot-Rooke, N., Le Pichon, X., Haines, A.J., Shen-Tu, B., Ren, J., 2000. Velocity field in Asia inferred from Quaternary fault slip rates and Global Positioning System observations. Journal of Geophysical Research 105, 19185–19209.
Hsieh, M.L., Chyi, S.J., 2010. Late Quaternary mass-wasting records and formation of fan terraces in the Chen-yeo-lan and Lao-nung catchments, central-south Taiwan. Quaternary Science Reviews 29, 1399–1418.
Hsieh, M.L., Knuepfer, P.L.K., 2001. Middle-late Holocene river terraces in the Erhjen river basin, southwestern Taiwan – implication of river response to climate change and active tectonic uplift. Geomorphology 38, 337–372.
Hsieh, M.-L., Rau, R.-J., 2009. Late Holocene coseismic uplift on the Hua-tung coast, Eastern Taiwan: evidence from mass mortality of interdital organisms. Tectonophysics 474 (3–4), 595–609.
Hsieh, M.-L., Lai, T.-H., Wu, L.-C., Liu, H.-T., Liew, P.M., 2006. Eustatic sea-level change of 11–5 ka in western Taiwan, constrained bu radiocarbon dates of core sediments. Terrestrial, Atmospheric and Ocean Sciences 17 (2), 353–370.
Hsu, Y.J., Yu, S.B., Simons, M., Kuo, L.C., Chen, H.Y., 2009. Interseismic crustal deformation in the Taiwan plate boundary zone revealed by GPS observations, seismicity, and earthquake focal mechanisms. Tectonophysics 479, 4–18.
Huang, M.-H., Hu, J.-C., Ching, K.-E., Rau, R.-J., Hsieh, C.-H., Pathier, E., Fruneau, B., Deffontaines, B., 2009. Active deformation of Tainan tableland of southwestern Taiwan based on geodetic measurements and SAR interferometry. Tectonophysics 466, 322–334.
Ivy-Ochs, S., Schaller, M., 2009. Examining processes and rates of landscape change with cosmogenic nuclides. Radioactivity in the Environment, vol. 16. Elsevier, pp. 231–294. doi:10.1016/S1569-4860(09)01606-4.
Korschinek, G., Bergmaier, A., Faestermann, T., Gerstmann, U.C., Knie, K., Rugel, G., Wallner, A., Dillmann, I., Dollinger, G., Lierse von Gosstomski, C., Kossert, K., Maiti, M., Poutivtsev, M., Remmert, A., 2010. A new value for the ^{10}Be half-life by heavy-ion elastic recoil detection and liquid scintillation counting. Nuclear Instruments & Methods 268, 187–191.
Lai, K.Y., Chen, Y.G., Hung, J.H., Suppe, J., Yue, L.F., Chen, Y.W., 2006. Surface deformation related to kink-folding above an active fault: evidence from geomorphic features and co-seismic slips. Quaternary International 147, 44–54.
Lal, D., 1991. Cosmic ray labeling of erosion surfaces: in situ nuclide production rates and erosion models. Earth Planetary Science Letters 104, 424–439.
Le Beon, M., Jaiswal, M.K., Ustaszewski, M.E., Suppe, J., Chen, Y.-G., 2010. Three Recipes to Decipher Late Pleistocene Slip Rates of the Chelungpu Thrust (Central Taiwan), Based on OSL-dated Folded Terraces, West Pacific Geophysical Meeting, Taipei, Taiwan, June 22–25, 2010 (Abstract).
Lee, T., You, C.-F., Liu, T.-K., 1993. Model-dependent ^{10}Be sedimentation rates for the Taiwan Strait and their tectonic significance. Geology 21 (5), 423–426.
Lee, J.C., Lu, C.Y., Chu, H.T., Delcaillau, B., Angelier, J., Deffontaines, B., 1996. Active deformation and paleostress analysis in the Pakua anticline area, western Taiwan. Terrestrial Atmospheric and Oceanic Sciences 7, 431–446.
Lee, T.Q., Lin, S.F., Chou, H.C., 1999. Preliminary magnetic study of the Quaternary red-soil bed on Linkou terrace, northern Taiwan. Terrestrial, Atmospheric and Oceanic Sciences 10, 763–776.
Lee, J.-C., Chen, Y.-G., Shieh, K., Mueller, K., Chen, W.-S., Chu, H.-T., Chan, Y.-C., Rubin, C., Yeats, R., 2001. A vertical exposure of the 1999 surface rupture of the Chelungpu Fault at Wufeng, Western Taiwan: structural and paleoseismic implications for an active thrust fault. Bulletin of the Seismological Society of America 91 (5), 914–929.
Liew, P.M., 1988. Quaternary stratigraphy in western Taiwan: palynological correlation. Proceedings Geological Society of China 31, 169–180.
Liew, P.-M., Pirazzoli, P.A., Hsieh, M.-L., Arnold, M., Barusseau, J.P., Fontugne, M., Giresse, P., 1993. Holocene tectonic uplift deduced from elevated shorelines, eastern Coastal Range of Taiwan. Tectonophysics 222 (1), 55–68.
Lifton, N.A., Bieber, J.W., Clem, J.M., Duldig, M.L., Evenson, P., Humble, J.E., Pyle, R., 2005. Addressing solar modulation and long-term uncertainties in scaling secondary cosmic rays for in situ cosmogenic nuclide applications. Earth and Planetary Science Letters 239 (1–2), 140–161.
Lu, H.H., Burbank, D.W., Li, Y.L., 2010. Alluvial sequence in the north piedmont of the Chinese Tian Shan over the past 530 kyr and its relationship to climate change. Palaeogeography, Palaeoclimatology, Palaeoecology 285, 343–353.
Maddy, D., Bridgland, D., Westaway, R., 2001. Uplift-driven valley incision and climate-controlled river terrace development in the Thames Valley, UK. Quaternary International 79, 23–36.
Maejima, Y., Nagatsuka, S., Higashi, T., 2002. Application of the crystallinity ratio of free iron oxydes for dating soils developed on the raised coral reef terraces of Kikai and Minami-Daito Island, southwest Japan. Quaternary Research 41, 485–493.
Malavieille, J., 2010. Impact of erosion, sedimentation and structural heritage on the structure and kinematics of orogenic wedges: analog models and case studies. Geological Society of America, Account GSA Today 20 (1), 4–10.
Malavieille, J., Lallemand, S.E., Dominguez, S., Deschamps, A., Lu, C.-Y., Liu, C.-S., Schnürle, P., and the ACT Scientific Crew, 2002. Arc-continent collision in Taiwan: new marine observations and tectonic evolution. In: Byrne, T.B., Liu, C.-S. (Eds.), Geology and Geophysics of an Arc-Continent Collision, Taiwan: Geological Society of America Special Paper 358, pp. 187–211.
Masarik, J., Frank, M., Schäfer, J.M., Wieler, R., 2001. Correction of in situ cosmogenic nuclide production rates for geomagnetic field intensity variations during the past 800,000 years. Geochimica et Cosmochimica Acta 65 (3–4), 515–521.
Massonnet, D., Feil, K.L., 1998. Radar interferometry and its application to changes in the Earth's surface. Reviews of Geophysics 36, 441–500.
Matsushi, Y., Wakasa, S., Matsuzaki, H., Matsukura, Y., 2006. Long-term denudation rates of actively uplifting hillcrests in the Boso Peninsula, Japan, estimated from depth profiling of in situ-produced cosmogenic ^{10}Be and ^{26}Al. Geomorphology 82, 283–294.
Merchel, S., Arnold, M., Aumaître, G., Benedetti, L., Bourlès, D.L., Braucher, R., Alfimov, V., Freeman, S.P.H.T., Steier, P., Wallner, A., 2008. Towards more precise ^{10}Be and ^{36}Cl data from measurements at the 10–14 level: influence of sample preparation. Nuclear Instruments and Methods in Physics Research Section B: Beam Interactions with Materials and Atoms 266 (22), 4921–4926.
Merritts, D.J., Vincent, K.R., Wohl, E.E., 1994. Long river profiles, tectonism, and eustasy: a guide to interpreting fluvial terraces. Journal of Geophysical Research 99, 14031–14050.
Middleton, R., Brown, L., Dezfouly-Arjomandy, B., Klein, J., 1993. On ^{10}Be standards and the half-life of ^{10}Be. Nuclear Instruments and Methods in Physics Research Section B: Beam Interactions with Materials and Atoms 82 (3), 399–403.
Molnar, P., Brown, E.T., Burchfiel, B.C., Deng, Q.D., Feng, X.Y., Li, J., Raisbeck, G.M., Shi, J.B., Wu, Z.M., Yiou, F., You, H.C., 1994. Quaternary climate change and the formation of river terraces across growing anticlines on the north flank of the Tian Shan, China. Journal of Geology 102, 583–602.
Mouthereau, F., Lacombe, O., Deffontaines, B., Angelier, J., Chu, H.T., Lee, C.T., 1999. Quaternary transfer faulting and belt front deformation at Pakuashan (western Taiwan). Tectonics 18 (2), 215–230.
Mouthereau, F., Fillon, C., Ma, K.-F., 2009. Distribution of strain rates in the Taiwan orogenic wedge. Earth and Planetary Science Letters 284, 361–385.

Please cite this article in press as: Siame, L.L., et al. Pleistocene alluvial deposits dating along frontal thrust of Changhua Fault in western Taiwan: The cosmic ray exposure point of view. Journal of Asian Earth Sciences (2012), doi:10.1016/j.jseaes.2012.02.002

Ng, S.M., Angelier, J., Chang, C.P., 2009. Earthquake cycle in Western Taiwan: insights from historical seismicity. Geophysical Journal International 178, 753–774.

Nishiizumi, K., Imamura, M., Caffee, M., Southon, J., Finkel, R., McAnich, J., 2007. Absolute calibration of Be-10 AMS standards. Nuclear Instruments and Methods in Physics Research Section B: Beam Interactions with Materials and Atoms 258, 403–413.

Oskin, M., Perg, L., Blumentritt, D., Mukhopadhyay, S., Iriondo, A., 2007. Slip rate of the Calico fault: implications for geologic versus geodetic rate discrepancy in the Eastern California Shear Zone. Journal of Geophysical Research 112, B03402.

Ota, Shyu, B.H., Chen, Y.G., Hsieh, M.L., 2002. Deformation and age of fluvial terraces south of the Choushui River, central Taiwan, and their tectonic implications. Western Pacific Earth Sciences 2, 251–260.

Ota, Y., Chen, Y.G., Chen, W.S., 2005. Review of paleoseismological and active fault studies in Taiwan in the light of the Chichi earthquake of September 21, 1999. Tectonophysics 408, 63–77.

Ota, Y., Lin, Y.N.N., Chen, Y.G., Chang, H.C., Hung, J.H., 2006. Newly found Tunglo Active Fault System in the fold and thrust belt in northwestern Taiwan deduced from deformed terraces and its tectonic significance. Tectonophysics 417 (3–4), 305–323.

Ota, Y., Lin, Y.N.N., Chen, Y.G., Matsuta, N., Watanuki, T., Chen, Y.W., 2009. Touhuanping Fault, an active wrench faut within fold-and-thrust belt in northwestern Taiwan, documented by spatial analysis of fluvial terraces. Tectonophysics 474, 559–570.

Pazzaglia, F.J., Gardner, T.W., Merritts, D.J., 1998. Bedrock fluvial incision and longitudinal profile development over geologic time scales determined by fluvial terraces. In: Wohl, E., Tinkler, K. (Eds.), Bedrock Channels. American Geophysical Union. Geophysical Monograph Series 107, Washington, pp. 207–235.

Pigati, J.S., Nifton, N.A., 2004. Geomagnetic effects on time-integrated cosmogenic nuclide production with emphasis on in situ ^{14}C and ^{10}Be. Earth and Planetary Science Letters 226 (1–2), 193–205.

Preusser, F., Chithambo, M.L., Götte, T., Martini, M., Ramseyer, K., Sendezera, E.J., Susino, G.J., Wintle, A.G., 2009. Quartz as a natural luminescence dosimeter. Earth-Science Reviews 97, 196–226.

Ritz, J.F., Brown, E.T., Bourlès, D.L., Philip, H., Schlupp, A., Raisbeck, G.M., Yiou, F., Enkhtuvshin, B., 1995. Slip rates along active faults estimated with cosmic-ray-exposure dates: application to the Bogd fault, Gobi-Altaï, Mongolia. Geology 23, 1019–1022.

Rixhon, G., Braucher, R., Bourlès, D., Siame, L., Bovy, B., Demoulin, A., 2011. Quaternary river incision in NE Ardennes (Belgium): insights from $^{10}Be/^{26}Al$ dating of river terraces. Quaternary Geochronology 6, 273–284.

Ryerson, F.J., Tapponnier, P., Finkel, R.C., Mériaux, A.-S., Van der Woerd, J., Lasserre, C., Chevalier, M.-L., Xu, X.-M., Li, H.-B., King, G.C.P., 2006. Applications of morphochronology to the active tectonics of Tibet. In: Lionel, L., Siame, Didier L. Bourlès, Brown, Erik T. (Eds.), In Situ-Produced Cosmogenic Nuclides and Quantification of Geological Processes. Geological Society of America Special Paper 415, Boulder, USA, 158 p.

Schaller, M., Hovius, N., Willett, S.D., Ivy-Ochs, S., Syna, H.-A., Chen, M.-C., 2005. Fluvial bedrock incision in the active mountain belt of Taiwan from in situ-produced cosmogenic nuclides. Earth Surface Processes and Landforms 30, 955–971.

Schmidt, S., Hetzel, R., Kuhlmann, J., Mingorance, F., Ramos, V.A., 2011. A note of caution on the use of boulders for exposure dating of depositional surfaces. Earth and Planetary Science Letters 302 (1–2), 60–70.

Schumm, S.A., 1977. The Fluvial System. John Wiley, New York, pp. 1–211.

Sella, G.F., Dixon, T.H., Mao, A., 2002. REVEL: a model for recent plate velocities from space geodesy. Journal of Geophysical Research 107 (B4). doi:10.1029/2000JB000033.

Shyu, J.B.H., Sieh, K., Chen, Y.-G., Liu, C.-S., 2005. Neotectonic architecture of Taiwan and its implications for future large earthquakes. Journal of Geophysical Research 110, B08402.

Shyu, J.B.H., Sieh, K., Chen, Y.-G., Chung, L.-H., 2006. Geomorphic analysis of the Central Range fault, the second major active structure of the Longitudinal Valley suture, eastern Taiwan. Geological Society of America Bulletin 118, 1447–1462.

Siame, L.L., Bourlès, D.L., Sébrier, M., Bellier, B., Castano, J.C., Araujo, M., Perez, M., Raisbeck, G.M., Yiou, F., 1997. Cosmogenic dating ranging from 20 to 700 ka of a series of alluvial fan surfaces affected by the El Tigre fault, Argentina. Geology 25 (11), 975–978.

Siame, L., Bellier, O., Braucher, R., Sebrier, M., Cushing, M., Bourlès, D., Hamelin, B., Baroux, E., de Voogd, B., Raisbeck, G., Yiou, F., 2004. Local erosion rates versus active tectonics: cosmic ray exposure modelling in Provence (south-east France). Earth and Planetary Science Letters 220, 345–364.

Siame, L.L., Bellier, O., Sébrier, M., Araujo, M., 2005. Deformation partitioning in flat subduction setting: the case of the Andean foreland of Western Argentina (28–33°S). Tectonics 24, 1–24.

Siame, L.L., Bourlès, D.L., Brown, E.T., 2006. In Situ-Produced Cosmogenic Nuclides and Quantification of Geological Processes: Preface. Special Paper of the Geological Society of America: Preface 415, pp. v–vi.

Siame, L.L., Chu, H.-T., Carcaillet, J., Lu, W.-C., Bourlès, D.L., Braucher, R., Angelier, J., Dussouliez, P., 2007. Glacial retreat history of Nanhuta Shan (North-east Taiwan) from preserved glacial features: the Cosmic ray exposure perspective. Quaternary Science Reviews 26, 2185–2200.

Siame, L.L., Angelier, J., Chen, R.-F., Godard, G., Derrieux, F., Bourlès, D.L., Braucher, R., Chang, K.-J., Chu, H.-T., Lee, J.-C., 2010. Erosion rates in an active orogen (NE-Taiwan): a confrontation of cosmogenic measurements with river suspended loads. Quaternary Geochronology 6 (2), 246–260.

Simoes, M., Avouac, J.P., 2006. Investigating the kinematics of mountain building in Taiwan from the spatiotemporal evolution of the foreland basin and western foothills. Journal of Geophysical Research 111, B10401.

Simoes, M., Avouac, J.-P., Chen, Y.-G., Singhvi, A.K., Wang, C.-Y., Jaiswal, M., Chan, Y.-C., Bernard, S., 2007. Kinematic analysis of the Pakuashan fault tip fold, west central Taiwan: shortening rate and age of folding inception. Journal of Geophysical Research 112, B03S14. doi:10.1029/2005JB004198.

Stein, R., Barka, A., Dieterich, J.H., 1997. Progressive failure on the North Anatolian Fault since 1939 by earthquake stress triggering. Geophysical Journal International 128, 594–604.

Stone, J.O., 2000. Air pressure and cosmogenic isotope production. Journal of Geophysical Research 105, 23753–23759.

Stone, J.O., Evans, J.M., Fiffeld, L.K., Allan, G.L., Cresswell, R.G., 1998. Cosmogenic chlorine-36 production in calcite by muons. Geochimica et Cosmochimica Acta 62, 433–454.

Streig, A.R., Rubin, C.M., Chen, W.-S., Chen, Y.-G., Lee, L.-S., Thompson, S.C., Madden, C., Lu, S.-T., 2007. Evidence for prehistoric coseismic folding along the Tsaotung segment of the Chelungpu Fault near Nan-tou, Taiwan. Journal of Geophysical Research – Solid Earth 112 (B3), B03S06.

Sung, Q.C., Lu, M.T., Tsai, H., Liu, P.M., 1997. Discussion on the genetics and the correlation of river terraces in Taiwan. Journal of Geological Society of China 40, 31–46.

Suppe, J., 1981. Mechanics of mountain building in Taiwan. Memoir of the Geological Society of China 4, 67–89.

Suppe, J., Connors, C.D., Zhang, Y.K., 2004. Shear fault-bend folding. In: McClay, K. (Ed.), Thrust Tectonics and Hydrocarbon Systems: AAPG Memoir 82, pp. 303–323.

Teng, L.S., 1987. Stratigraphic records of the late Cenozoic Penglay orogeny of Taiwan. Acta Geologica Taiwanica 25, 205–224.

Tsai, H., Huang, W.S., Hseu, Z.Y., Chen, Z.S., 2006. A river terrace soil chronosequence of the Pakua tableland in Taiwan. Soil Science 171, 167–179.

Tsai, H., Hseu, Z.Y., Huang, W.S., Chen, Z.S., 2007a. Pedogenic approach to resolving the geomorphic evolution of the Pakua river terraces in central Taiwan. Geomorphology 83, 14–28.

Tsai, H., Huang, W.-S., Hseu, Z.-Y., 2007b. Pedogenic correlation of lateritic river terraces in central Taiwan. Geomorphology 88, 201–213.

Tsai, H., Maejima, Y., Hseu, Z.Y., 2008. Meteoric ^{10}Be dating of highly weathered soils from fluvial terraces in Taiwan. Quaternary International 188, 185–196.

Tsai, H., Hseu, Z.-Y., Huang, S.-T., Huang, W.-S., Chen, Z.-S., 2010. Pedogenic properties of surface deposits used as evidence for the type of landform formation of the Tadu tableland in central Taiwan. Geomorphology 114, 590–600.

Van der Woerd, J., Ryerson, F.J., Tapponnier, P., Gaudemer, Y., Finkel, R.C., Mériaux, A.-S., Caffee, M.W., Zhao, G., He, G., 1998. Holocene left-slip rate determined by cosmogenic surface dating on the Xidatan segment of the Kunlun fault (Qinghai, China). Geology 26, 695–698.

Vita-Finzi, C., 2000. Deformation and seismicity of Taiwan. Proceedings of the National Academy of Sciences of the United States of America 97 (21), 11176–11180.

von Blanckenburg, F., 2005. The control mechanisms of erosion and weathering at basin scale from cosmogenic nuclides in river sediment. Earth and Planetary Science Letters 237, 462–479.

von Blanckenburg, F., Hewawasam, T., Kubik, P.W., 2004. Cosmogenic nuclide evidence for low weathering and denudation in the wet, tropical highlands of Sri Lanka. Journal of Geophysical Research 109, 1–22.

Walker, J.P.F., Roberts, G.P., Sammonds, P.R., Cowie, P.A., 2010. Comparison of earthquake strains over 10(2) and 10(4) year timescales: insights into variability in the seismic cycle in the central Apennines, Italy. Journal of Geophysical Research: Solid Earth 15, ISSN 0148-0227.

Walters, R.J., Holley, R.J., Parsons, B., Wright, T.J., 2011. Interseismic strain accumulation across the North Anatolian Fault from Envisat InSAR measurements. Geophysical Research Letters 38, L05303. doi:10.1029/2010GL046443.

Wei, M., Sandwell, D., Fialko, Y., Bilham, R., 2011. Slip on faults in the Imperial Valley triggered by the 4 April 2010 Mw 7.2 El Mayor-Cucapah earthquake revealed by InSAR. Geophysical Research Letters 38, L01308. doi:10.1029/2010GL045235.

Westaway, R., 1992. Seismic Moment Summation for Historical Earthquakes in Italy: tectonic implications. Journal of Geophysical Research 97 (B11), 15437–15464.

Wintle, A.G., 2008. Luminescence dating of Quaternary sediments – introduction. Boreas 37, 469–470.

Wintle, A.G., Murray, A.S., 2006. A review of quartz optically stimulated luminescence characteristics and their relevance in single-aliquot regeneration dating protocols. Radiation Measurements 41, 369–391.

Wolkowinsky, A.J., Granger, D.E., 2004. Early Pleistocene incision of the San Juan River, Utah, dated with ^{26}Al and ^{10}Be. Geology 32, 749–752.

Wu, T.-S., Jaiswal, M.K., Lin, Y.-W., Chen, Y.-W., Chen, Y.-G., 2010. Residual luminescence in modern debris flow deposits from Western Taiwan: a single grain approach. Journal of Asian Earth Sciences 38 (6), 274–282.

Yamaguchi, M., Ota, Y., 2001. Tectonic interpretation of Holocene marine terraces, east coast of Coastal Range, Taiwan. Quaternary International 115, 71–81.

Yang, G.F., Zhang, X.J., Tian, M.Z., Brierley, G., Chen, A.Z., Ping, Y.M., Ge, Z.L., Ni, Z.Y., Yang, Z., 2011. Alluvial terrace systems in Zhangjiajie of northwest Hunann China: implications for climatic change, tectonic uplift and geomorphic evolution. Quaternary International 233, 27–39.

Please cite this article in press as: Siame, L.L., et al. Pleistocene alluvial deposits dating along frontal thrust of Changhua Fault in western Taiwan: The cosmic ray exposure point of view. Journal of Asian Earth Sciences (2012), doi:10.1016/j.jseaes.2012.02.002

Yen, I.-C., Chen, W.-S., Yang, C.-C.B., Huang, N.-W., Lin, C.-W., 2009. Paleoseismology of the Rueisuei segment of the Longitudinal Valley Fault, Eastern Taiwan. Bulletin of the Seismological Society of America 98 (4), 1737–1749.

Yu, S.B., Chen, H.Y., Kuo, L.C., 1997. Velocity field of GPS stations in the Taiwan area. Tectonophysics 274, 41–59.

Yue, L.F., Suppe, J., Hung, J.H., 2005. Structural geology of a classic thrust belt earthquake: the 1999 Chi–Chi earthquake Taiwan (Mw7.6). Journal of Structural Geology 27, 2058–2083.

Yue, L.F., Suppe, J., Hung, J.H., 2009. Two contrasting kinematics styles of active folding above thrust ramps, western Taiwan. In: McKlay, K., Shaw, J., Suppe, J. (Eds.), Thrust Fault-related Folding. American Association of Petroleum Geologists Memoir 94, pp. 1–34.

Please cite this article in press as: Siame, L.L., et al. Pleistocene alluvial deposits dating along frontal thrust of Changhua Fault in western Taiwan: The cosmic ray exposure point of view. Journal of Asian Earth Sciences (2012), doi:10.1016/j.jseaes.2012.02.002